Department of Chemistry
Inorganic Chemistry
Royal Institute of Technology
S-100 44 Stockholm Sweden

ISSN 0348-825x
TRITA-OOK 1051

Constitution, Dynamics and Structure of Binary and Ternary Actinide Complexes

Wenche Aas

AKADEMISK AVHANDLING

som med tillstånd av Kungliga Tekniska Högskolan framlägges till offentlig granskning för avläggande av filosofie doktorsexamen i oorganisk kemi, måndagen den 29 mars 1999, kl 10.00 i kollegiesalen, Valhallavägen 79, KTH. Fakultetsopponenten är Professor Norman Edelstein, Lawrence Berkley National Laboratory, USA. Avhandlingen försvaras på engelska.

Abstract

Stoichiometry, ligand exchange reactions, coordination geometry and stability of complexes of type $UO_2L_pF_q(H_2O)_{3-n}$ (p = 1 – 2, q = 1-3), where L is one of the bidentate ligands picolinate, oxalate, carbonate or acetate have been investigated using single crystal X-ray diffraction, an array of ^{19}F-, ^{13}C-, ^{17}O- and ^{1}H-NMR techniques and potentiometric titration using both F^- and H^+ selective electrodes. The experiments were performed in a 1.00 M $NaClO_4$ medium. The equilibrium constants were determined at 25°C while most of the kinetic experiments were done at - 5°C. The equilibrium constants for the stepwise addition of F^- to UO_2L and UO_2L_2 indicates that the prior coordination of L to U(VI) has a fairly small effect on the subsequent bonding of fluoride, except for a statistical effect determined by the number of available coordination sites. This indicates that ternary complexes might be important for the speciation and transport of hexavalent actinides in ground and surface water systems. A single crystal structure of UO_2(picolinate)F_3^{2-} has been determined showing the same pentagonal bipyramidal symmetry as in aqueous solution studied by NMR. The exchangeable donor atoms are situated in a plane perpendicular to the linear uranyl group. The complexes show a variety of different exchange reactions depending on the ligand used. It has been possible to quantify external fluoride and the other ligands exchange reactions as well as *intra*-molecular reactions. This type of detailed information has not been observed in aqueous solution before. Water takes a critical part in the exchange mechanism, and when it is eliminated from the inner coordination sphere a much slower kinetics can be observed. ^{19}F-NMR has showed to be a powerful technique to study these reactions, both because of the sensitivity of this NMR nucleus and also the possibility to observe reactions where fluoride is not directly involved in the mechanism. Ternary Th(edta)F_{1-2} and $(UO_2)_2$(edta)$_2F_{1-4}$ have been investigated using ^{1}H and ^{19}F-NMR. The fluoride complexation to Cm(III) was studied using time resolved fluorescence spectroscopy (TRLFS) and the stability constant for the CmF^{2+} complex was determined at 25°C in 1.0 m NaCl.

Keywords. Ternary complexes, actinides, dioxouranium(VI), curium(III), thorium(IV), ligand exchange, isomers, NMR, potentiometric titrations, aqueous solution, oxalate, picolinate, acetate, EDTA.

Preface

I started the work on this thesis 1st of April 1995, and it has been carried out at the Department of Chemistry, Institute of Inorganic Chemistry at the Royal Institute of Technology (KTH) in Stockholm and supervised by Professor Ingmar Grenthe. Six weeks work were done at the Research Centre Karlsruhe (FZK), supervised by Dr. Thomas Fanghänel. The thesis is based on the following manuscripts:

Paper I "Structure, Isomerism, and Ligand Dynamics in Dioxouranium(VI) Complexes"
Zoltán Szabó, Wenche Aas and Ingmar Grenthe
Inorganic Chemistry **1997**, *36*, 5369-5375.

Paper II "Complex Formation in the Ternary U(VI)-F-L System (L = Carbonate, Oxalate, and Picolinate)"
Wenche Aas, Alexander Moukhamet-Galeev and Ingmar Grenthe
Radiochimica Acta **1998**, *82*, 77-82.

Paper III "Thermodynamics of Cm(III) in concentrated electrolyte solutions. Fluoride complexation in I = 1 m NaCl at 25°C"
Wenche Aas, Elke Steinler, Thomas Fanghänel and Jae Il Kim
Radiochimica Acta, in press, 1999.

Paper IV "Equilibrium and Dynamics in the binary and ternary uranyl(VI) oxalate and acetate / fluoride complexes"
Wenche Aas, Zoltán Szabó and Ingmar Grenthe
Journal of Chemical Society, Dalton transactions, accepted, 1999

Paper V "Structure of the sodium salt of the ternary uranyl-picolinate-fluoride complex: $[UO_2(picolinate)F_3]Na_2(H_2O)_4$"
Wenche Aas and Maria H. Johansson
Acta Chemica Scandinavica, submitted 1999.

Appendix "A tentative study of the dynamics in ternary Th(IV) and U(VI) EDTA complexes.
Wenche Aas
A manuscript based on still not completed work.

Table of Contents

I Introduction

Solution coordination chemistry is an old established research area [1,2] with its origin from last century. It includes constitution, geometry and reactivity of various metal complexes. The work presented in this thesis deals with the coordination chemistry of some actinide elements in aqueous solution, and it covers a number of fundamental chemical properties of the investigated systems. Knowledge of this type is necessary to verify existing, or to develop new, scientific theories. It is essential to understand these chemical properties when applying them in other areas, such as the field of nuclear technology. The chemical theories may for example be used to develop separation techniques, a crucial step in the processing of spent nuclear fuel. Another important application is to use solution data to judge whether the actinides may migrate from nuclear waste repositories through transport in surface and groundwater systems. These questions are essential, *e.g.* in the construction and safety assessment of systems for the final storage of radioactive wastes.

The actinide elements have noticeably different properties from the *d*- and 4*f*-elements; this is due to the electron structure of the 5*f*-elements. The 5*f*-electrons can participate in bonding, in contrast to the 4*f*-electrons that are more shielded and essentially part of the core. A typical example is the formation of the linear $MO_2^{+/2+}$ ion. These linear dioxocations are unique to the actinides; they are only found for the elements U, Np, Pu and Am. The actinides are radioactive, and the chemistry of many of the elements, at least for the trans-uranium elements, is therefore difficult to study experimentally. The 5*f*-elements can attain several oxidation states, from +2 to +7, in contrast to the lanthanides where oxidation state +3 is the most common. But, like the lanthanides, the elements with the same oxidation state have very similar chemical properties. This makes it possible to use the chemical properties of selected actinides, in my case Cm(III), Th(IV) and U(VI), to obtain general information on other actinides of oxidation states III, IV and VI. The cations of oxidation states II to VI normally exist as M^{2+}, M^{3+}, M^{4+}, MO_2^{+}, MO_2^{2+}. These ions are electron acceptors and their affinity to different ligands usually increases with charge. However, the effective charges on the MO_2^{+} and MO_2^{2+} ions are higher than the ionic charge; hence, the tendency to form complexes decreases in the order $M^{4+} > MO_2^{2+} > M^{3+} > MO_2^{+}$.

The main themes of the thesis are divided into three parts: constitution, coordination geometry and chemical dynamics.

- **Constitution**. This part of the thesis discusses the stoichiomety and equilibrium constants in aqueous solution of the chosen actinide systems. It concerns mainly an analytical problem. A special technique has to be used to determine the constitution in a chemical system where the components are in fast equilibrium with one another and the constituents cannot be separated and analysed individually. The technique is well established, and it is described for example by Rossotti and Rossotti [3]. Most of the literature data on the actinides concerns primarily binary complexes [4,5]. When considering a natural aquatic environment, there are many potential complexing ligands, and it is therefore more probable that complexes with two or more ligands are formed. It is not possible to study the enormous number of potential ternary or higher complexes that may be formed in the multi-component aquatic system in nature. It is therefore necessary to create theories and models to predict which combinations of ligands are more probable than others and use this information to guide the selection of systems for experimental study. We can judge which species are more likely to form strong complexes by using for example the concept of hard/soft donor and acceptor groups. These theories can be extended, using the knowledge of the coordination geometry of the ligands and central metal ion. From these theories, one would expect that ternary complexes in ground and surface water systems might contain fluoride as one of the ligands. Fluoride is a typical hard donor, binding strongly to the actinides. Since it is a single atom donor, it does not have strict geometrical requirements for binding; it is also small and demands little space. An experimental advantage of studying fluoride systems is that a fluoride selective electrode can be used in the equilibrium studies. In addition, fluoride has a nuclear spin ½ and a high NMR sensitivity. The identified ternary complexes will be compared with the properties of the corresponding binary systems. One question that will be discussed is how an additional coordinated ligand will influence the size of the stepwise formation constants.

- **Coordination geometry**. Classical determinations of equilibrium data, in general do not contain information on isomers and their relative stability. Information of this type, in dynamic systems, can only be obtained if the exchange between the individual isomers is slow in comparison to the time resolution of the technique used. The classical example is Niels Bjerrums study of stepwise equilibrium in the chromium(III) thiocyanate system [6,7]. Identification of isomers is important because it allows us to identify the geometry around the central metal ion. Fast isomerisation reactions must be studied using a technique with fast detection limits, for example spectroscopy such as NMR in our case. The time scale that can be studied is dependent on the chemical shift difference between the species. This makes ^{19}F-NMR very promising, because there are often large chemical shift differences between fluorides in different environments. NMR also has the advantage of providing symmetry information on the complexes studied. This information is important for identifying, for example, the coordination mode of a ligand and the coordination geometry of the complex. There are often large similarities between the coordination geometry in solution and solid state. We have therefore crystallised one complex and determined the crystal structure to obtain insight into its structure in solution. Single crystal X-ray diffraction is the most important technique to study solid structures. This makes it possible to obtain a more precise determination of the coordination geometry, than is possible in solution.

- **Chemical dynamics**. A complex formation reaction is a substitution of a coordinated solvent molecule with another ligand. These reactions can take place in several different ways, where the main classifications are dissociative, associative or interchange mechanisms [8]. Very little is known of the dynamics in actinide systems in general, and in ternary systems in particular. It has for example never been possible to identify different isomers in aqueous solution. In an earlier uranyl-fluoride study [9], there were indications that the ligand exchange rates and mechanisms are influenced by the number of water molecules in the inner coordination sphere. The coordinated water was therefore replaced with other ligands, in an attempt to slow down the exchange processes and

thereby possibly obtain more detailed information of the different exchange mechanisms. Questions that will be discussed are whether the reactions take place in one or several steps, if there are parallel pathways and the intimate mechanism for exchanging a chelating ligand. Another point will be to compare the exchange rates and mechanisms in the binary and ternary systems.

The main work has been performed on U(VI), but also Cm(III) and Th(IV) systems have been investigated. These metals have different properties and combined, they represent most of the characteristics of the actinide elements. The ligands that are chosen are carbonate, oxalate, fluoride, picolinate, EDTA, and acetate. The first three ligands are present in natural water systems depending on the local geology. The other three are used to illustrate the different properties of unsymmetrical, large chelating or a weak coordinating ligand, respectively. It has been necessary to use an array of different techniques: multinuclear NMR spectroscopy, potentiometric titrations, fluorescence spectroscopy, and single crystal X-ray diffraction. These will be described in a separate chapter while each of the three main areas listed above will be described in individual chapters.

II Experimental Methods

The objectives of this thesis cover several topics. To be able to study the stability, dynamic and structural properties of the actinides, it has been necessary to use several techniques. This chapter describes the general principles and background of the methods used.

2.1 Methods for studying solution chemical equilibria

A solvated metal ion (M^{n+}), together with one or more potential ligands (L) may react and form complexes of type M_qL_p, where L has substituted one or more of the coordinated solvent molecules. The stability of this complex is defined by its stability constant ($\log\beta_{pq}$). The charges are left out in the general expressions for simplicity.

$$pM + qL \leftrightarrows M_pL_q \qquad (2.1)$$

$$\beta_{pq} = \frac{[M_pL_q]}{[M]^p[L]^q} \qquad (2.2)$$

The convention (IUPAC) is to use the notation β for the overall stability constant, while K is used when referring to a stepwise constant. To determine these constants, it is necessary to know the concentrations of the species in the equation. One might be able to identify concentrations of the individual species using different spectroscopic methods (discussed later), but utilising potentiometry, this is often not feasible. However, there are ways of deriving both the stoichiometric composition and the desired constants without *direct* information of all separate concentrations. This can be achieved by using the total concentrations of the different components and the equilibrium concentrations of at least one reactant / product. Rossotti and Rossotti [3] wrote in 1960 a classical book, still very much in use, on how to determine stability constants by different techniques. At that time, potentiometry was one of the main, and certainly the most precise, experimental methods.

2.1.1 Background for classical analysis using potentiometry

The ligands are usually Brønsted bases and their protonation is therefore a competing reaction to the complexation. If the corresponding acid is monoprotic, the total amount of protons in the solution is

$$[H^+]_{total} = [H^+]_{free} + [HL] = [H^+]_{free} + K_{HL}[H^+]_{free}[L^-] \quad (2.3)$$

where K_{HL} is the protonation constant. The free proton concentration can easily be determined potentiometrically using for example a glass or quinhydron electrode. When the total amount of protons is known, the free ligand concentration can be calculated.

$$[L^-] = \frac{[H^+]_{total} - [H^+]_{free}}{K_{HL}[H^+]_{free}} \quad (2.4)$$

The total ligand concentration is the sum of the free ligand and the amount of complexed ligand. One approach to calculate the formation constant in equation 2.2 is to create a $\bar{n}$ function, which is the average number of coordinated ligands per metal ion. For illustration and simplicity, the coefficient *p* and *q* are set to 1.

$$\bar{n} = \frac{[L]\,\text{bonded to M}}{[M]_{total}} = \frac{[L]_{total} - [L] - [HL]}{[M]_{total}} \quad (2.5)$$

or

$$\bar{n} = \frac{[ML]}{[M]_{total}} = \frac{\beta_{11}[M][L]}{[M] + [ML]} = \frac{\beta_{11}[L]}{1 + \beta_{11}[L]} \quad (2.6)$$

The expression (2.5) and (2.6) can be arranged in several ways to obtain the formation constant graphically. An example would be a linear plot. The situation is more complicated if several complexes are formed, for polyprotic acids and polynuclear species, but the principles are the same; the known total concentrations of ligand, proton and metal in addition to the measured -log[H^+] are used to obtain the ligand concentration and to calculate the $\bar{n}$ function. Sometimes it is possible to use an ion selective electrode to measure directly the free metal (*e.g.* Cd^{2+},Cu^{2+} Ca^{2+}) or ligand (*e.g.* Cl^-, F^-) concentrations, this will certainly simplify the evaluation of complicated systems. The total set of measured data is usually treated with a least square program. There are several programs available, most of them are based on LETAGROP, written in 1958 by Sillén and coworkers [10]. This was the first to use the so-called “pit mapping” method. The best model is usually defined [11] to be the one that gives a minimum value to an error square sum, U, for an experimental quantity *y*, equation 2.7.

$$U = \sum w(y_{calc} - y_{exp})^2 \qquad \sigma^2(y) = U_{min}/(n_{obs}-n_{par}) \quad (2.7)$$

w refers to a weight factor, in our case chosen to be unity. When *w* = 1, as on our case, the standard deviation $\sigma^2(y)$ is as written above; n_{obs} is the number of observations and n_{par} is the number of parameters to be adjusted. The error carrying variable, *y,* can be chosen to be either one of the total or free concentrations in the $\bar{n}$ function. In our study, *y* is either the total proton or fluoride concentrations. The uncertainty in the minimisation function, U, is largest when the total and free concentrations are of same magnitude. Therefore one can derive a good fit, meaning a small U_{min}, but the real uncertainty might be larger than the estimated. This can be illustrated using the formation function (2.5). At high -log[H^+], the [HL] concentration is negligible, and when $[L]_{total} \approx [L]$, the uncertainty in $\bar{n}$ is large. It is necessary to be aware of this problem, otherwise one can easily obtain a wrong model. It is also important to estimate the concentrations of all complexes that are present. For example, one can always obtain a better fit by including more complexes in the model. However, if a complex is only present in a few percent, one should use additional experimental methods to be sure that it really exists and that it is not a computational artifact.

The activity coefficient. The equations written above are simplified by not considering the activity coefficients. The correct way of describing an equilibrium constant is to use the activity of the various species and not their concentrations. The activity is defined as $a_j = [j]\gamma_j$ where γ_j is the activity coefficient of species *j*. The activity coefficients are strongly dependent on the electrolyte concentration. By using an ionic medium of high and approximately constant ionic strength, the activity coefficient of reactants and products remain nearly constant when their total concentrations are varied. We may then define their activity coefficient as 1 in the medium used, and use concentrations instead of activities. This means that the numerical values of the formation constants (but in general not the stoichiometry of the complexes) are dependent on the ionic medium in which the measurements have been performed. Therefore, in addition to the equilibrium data, the conditions under which they were determined must be presented as well. It is necessary to recalculate the formation constants from one medium to another when using literature data obtained in other ionic media. There are several available models; most of them are based on the Debye-Hückel theory. The theory is usually extended, *e.g.* as in “specific ion interaction (SIT) method”, which consists of a Debye-Hückel term that takes into

account the long range electrostatic interaction and another term, a short-range non-electrostatic interaction term that is valid at high ionic strength. This approach was outlined by Brønsted and elaborated by Scatchard and Guggenheim; hence, the model is also called “The Brønsted – Guggenheim - Scatchard model”. The activity coefficient γ_j of species *j* of charges z_j is defined:

$$\log\gamma_j = -z_j^2 D + \sum_k \varepsilon_{(j,k)} m_k \qquad (2.8)$$

where, $\varepsilon_{(j,k)}$ are the SIT coefficients, that are summarised for all species *k* with molality m_k. It is important to notice that the ions *k*, are those in the ionic medium and not the ions in small concentrations, such as complexes, ligands *etc.* D is the Debye-Hückel term,

$$D = \frac{A\sqrt{I_m}}{1 + Ba_j\sqrt{I_m}} \qquad (2.9)$$

where A and B are temperature dependent constants and a_j is the effective diameter of the hydrated ion *j*. Estimated values for the Debye-Hückel parameters are to be found in literature [12,13], A is 0.51 and Ba_j is approximately 1.5 at 25^{O}C and 1 atm. The SIT coefficients have been measured or estimated for many ion pairs [13,14] using the assumption that they are concentration independent. This is valid at high molality, but the deviations can be large at lower concentrations. Concentration dependent ion interaction coefficients can be included in the equation. However, this variation is not so important since the product of $\varepsilon_{(j,k)} m_k$ only gives a small contribution at low ionic strength, *c.f.* equation 2.8. It is also assumed that the coefficient is zero for ions of same charge, and that the contribution from ternary interactions can be ignored. The short comings of the SIT model lead Pitzer to develop an extended model. It is more complicated containing three parameters compared to one for the SIT model. The Pitzer approach [13,15], can often give a better description of a multi-component system, at least in electrolytes at high ionic strength, but it requires a large number of empirical data which may be difficult to obtain. A detailed description of this model is given in the literature [13,15].

The liquid junction potential. The most common experimental setup for potentiometry is to use a cell containing two electrodes separated in solutions connected through a liquid-liquid junction [3]. The measured potential (E) contains a contribution from the liquid junction potential (E_j) in addition to the potential differences between the two half cells. This is caused by an unequal distribution of ions in the two solutions and the diffusion of the ions across the liquid junction will give rise to an additional potential. A modified Nernst equation can be written:

$$E = E^0 + \frac{RT}{nF} \ln C + E_j \qquad (2.10)$$

where E^0 is the standard potential, R is the gas constant, F is the Faraday's constant, C is the concentration term. The ionic medium is usually very near the same in the two cells during the measurements, but a large change in H^+ or OH^- can give rise to a significant diffusion potential. If the proton concentration is measured in the acidic region where the diffusion potential is due to a difference in proton concentration, equation 2.10 can be written as:

$$E = E^0 + g*\log[H^+] - j[H^+] \qquad (2.11)$$

where g is a constant including R, T and F, and *j* is the liquid junction coefficient. The diffusion potential is linear with respect to the concentration and the coefficient can easily be determined. If the ionic medium is changing throughout the experiment, a significant diffusion potential can arise. For example, when one of the ions in the electrolyte is replaced with a reactant, the electrolyte content in the two cells is no longer equal.

Limitations. Equilibrium analyses with potentiometry can give very good estimations of formation constants. Changes of only few micromolar in proton concentration are possible to detect depending on the precision of the electrodes and instruments. On the other hand, the stoichiometry of the complexes do not include information on number of solvent molecules in the coordination sphere or about the coordination geometry. For example, when two species of same stoichiometry are formed (isomers), an average value for their equilibrium constants will be determined. It is also important that the dynamics of the system is relatively fast,

which usually means that equilibrium should be reached within minutes. If equilibrium has not been reached, the observed potentials refer to non-equilibrated states.

2.1.2 Spectroscopic methods

Spectroscopy is a more direct method to obtain the concentration of the species involved in a complexation reaction compared to that of potentiometry. Utilising spectroscopy, the species may be directly observed in a spectrum. It provides an additional method for determining equilibrium constants and to decide on which chemical model is most consistent with experimental data. Evaluation of potentiometric data may result in precise formation constants even if the model is erroneous. This may also occur in a spectroscopic study; however, the possibility to directly observe each species is an obvious advantage. On the other hand, spectroscopic data are often less precise compared to those of potentiometry. Therefore, the two techniques are complementary and should be combined whenever possible. Comparing the spectroscopic methods ultraviolet-visible (UV-vis) and nuclear magnetic resonance (NMR), the first usually gives broad peaks, which contain contributions from all complexes formed. Whereas in NMR, the line broadening is usually much smaller and most important. The peaks from the complexes often do not overlap, at least for the common NMR nuclei ^{1}H, ^{13}C and ^{19}F. The difference can be explained by the different relaxation mechanism. The signals in absorption spectroscopy are dependent on the lifetime of the excited states and these are usually very short, hence broad signals. The exited species in NMR spectroscopy are usually long lived and therefore give rise to narrow signals.

NMR. In contrast to most other spectroscopic techniques, it is possible to determine both free and coordinated ligand concentrations from NMR spectra. Whether this is possible or not, depends on the chemical shift difference between the species and the rate of exchange between them. A more detailed discussion on how dynamic processes influence the NMR spectra is presented later in section 2.2.1. The integrals of the individual peaks are proportional to their concentration. The accuracy is dependent on the shape of the peak and the signal to noise ratio. It is common to work in a rather low concentration range. Furthermore a good baseline

correction is a necessity to achieve reliable data. This is of most importance if there are broad peaks that can be difficult to integrate since part of the peak may disappear into the baseline. When data are used for quantitative analysis, the absolute total intensity of all the peaks should checked against a standard with known concentration to ensure that a proper baseline correction has been made and that there are no peaks "hidden" in the baseline.

UV-vis. Due to the fast relaxation and small differences in the absorption wavelengths, the spectrum of a dynamic system usually contains the superimposed spectra of all individual spectra. The intensity of the absorption spectra is related to the concentration of the absorbing species (Beer-Lamberts law). Quantitative analysis can be accomplished when the spectrum can be deconvoluted into individual spectra. In situations where this is not possible, a similar approach as in the potentiometric techniques using the known total concentrations *etc.* may be applied. One way of improving the sensitivity is to measure the fluorescence or phosphorescence spectrum. The peaks are often less overlapping in emission spectra, and in many cases the detection limits are lower. The excitation of an electron takes place between equal spin states, while the fluorescence takes place between two different spin states. This will lead to long lived excited species; thus, the fluorescence spectroscopy is time dependent, which sometimes is an advantage. Time resolved laser fluorescence spectroscopy (TRLFS) has shown to be an excellent tool of high sensitivity to study curium(III) complexes in micromolal concentrations .

TRLFS applied on Cm(III). The excitation spectra of Cm(III) in the spectral range of 370-405 nm is given in Figure 2.1. There are three excitation bands, the F, G and H bands absorbing at 396.5, 381.1 and 374.4 nm, respectively. A dye laser was tuned to the maximum of the H band for excitation, and the emission band A was recorded. This band is strongly influenced by complexation usually observable as a red shift of the spectrum. The individual spectrum of each complex is usually not observable, but by deconvolution, all species present might be identified. The curium emission spectrum is in contrast to many other elements relatively simple. It contains only one peak for each Cm-species, which makes deconvolution rather easy.

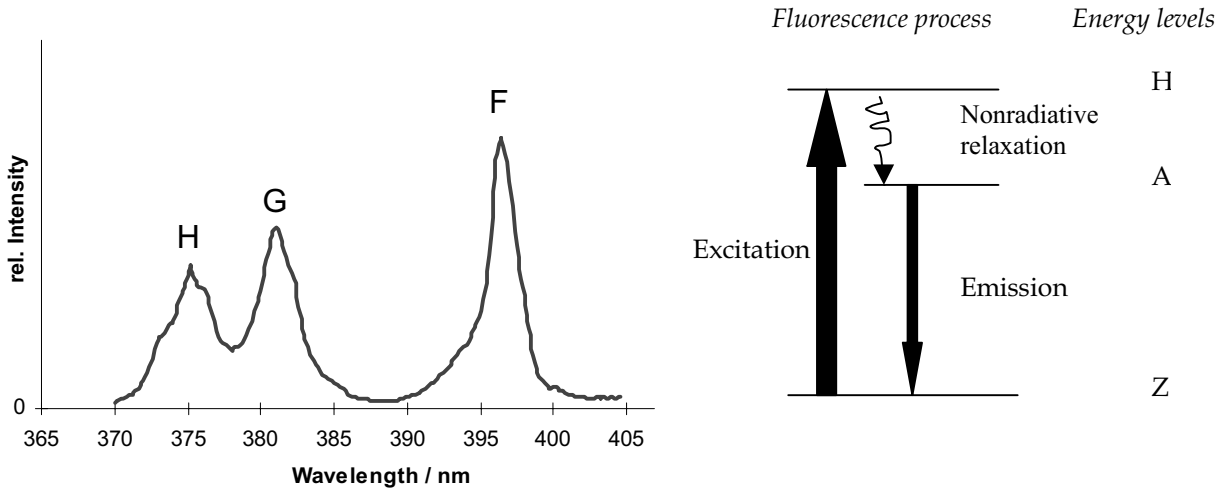

***Figure 2.1**. Excitation spectra of aqueous Cm^{3+} ion, and a schematic sketch of the fluorescence process.*

The non-radiative decay for the excited state is mainly due to energy transfer from the exited central atom to the ligand vibrators, *e.g.* O-H. The lifetime (τ) of the exited species is therefore strongly dependent on the coordination sphere around curium. The excited curium aqua ion has a relative short lifetime, 65 μs because of the fast quenching caused by O-H vibrations. This can be observed by measuring the lifetime in heavy water where it increases to 1270 μs due to the lower O-D vibration frequency [16]. When exchanging water with other ligands, the lifetime usually increases; for examples τ for $Cm(CO_3)_3^{3-}$ [17] and $Cm(SO_4)_3^{3-}$ [18] are 215 and 195 μs, respectively. A correlation between the reciprocal lifetimes and the numbers of coordinated water molecules has been made for Cm(III) doped in lanthanum compounds [16]. Based on this, the hydration number of the complex can be calculated from the measured lifetime. The possibility to measure both lifetime and fluorescence gives more specific information than absorption spectroscopy alone. When the time dependence of the fluorescence emission follows a mono exponential decay, it is a strong evidence that the ligand exchange reactions are faster than the relaxation rate, and that the system is in equilibrium both in the exited and ground states [19]. This is important if the fluorescence intensity is going to be used to determine equilibrium constants. The intensity of the signal is dependent on the lifetime of the species, but with a fast equilibrium all species present will give an intensity *ratio* which depends only on the equilibrium concentrations. It is the total

integral intensity alone that will be altered with a change in lifetime. The mole fraction of a given species is directly proportional to the relative intensity of its emission spectrum, equation 2.12

$$m_i = x_i m_{\mathrm{Cm(tot)}} = (I_i / I_{\mathrm{tot}}) m_{\mathrm{Cm(tot)}} \qquad (2.12)$$

where m_i and x_i are the molality and mole fraction, respectively, of species *i*, $m_{\mathrm{Cm(tot)}}$ the total molality of Cm(III), I_{tot} the total integral of the spectrum, and I_{i} the integral of species *i*. Assuming a mononuclear formation of complex CmL_n, the formation constant is then

$$\beta_{1n} = \frac{[\mathrm{CmL_n}]}{[\mathrm{Cm^{3+}}][\mathrm{L}]^n} \qquad (2.13)$$

or rewritten as

$$\log \frac{[\mathrm{CmL_n}]}{[\mathrm{Cm^{3+}}]} = \log\beta_{1n} + n\log[\mathrm{L}] \qquad (2.14)$$

The free ligand concentration is either measured or estimated by subtracting the bonded ligand concentration from the total concentration. Plotting the left side of equation 2.14 against log[L] the number of bonded ligands (*n*) is estimates from the slope, while the intercept is the formation constant.

2.2 Methods for studying dynamic systems

To deduce a reaction mechanism, it is necessary to measure how the rate of reaction depends on the concentration of the various species present and from this deduce a rate equation for the reaction of interest. Fast kinetic reactions have traditionally been studied using stopped flow or relaxation techniques. The flow techniques are limited by the rate of mixing two solutions; hence, only systems with half-life slower than ~10^{-3} s are feasible to study. With relaxation methods, a system at equilibrium is disturbed and the time for the system to reach equilibrium again is measured, usually with spectrophotometrical methods. It is possible to measure half-life down to 10^{-6} s with such techniques. Fast temperature changes are often used to disturb the system. Relaxation methods operate in real time by measuring the change in concentrations with time. Dynamic information might also be obtained for systems in equilibrium by the use of NMR spectroscopy. The increasing sensitivity of NMR and the use of various pulse sequences has made NMR a very effective instrument for

obtaining kinetic data. The advantage of using NMR for dynamic studies lies also in the possibility to operate on different time scales as described below.

2.2.1 Dynamic NMR spectroscopy [20,21].

In non-equilibrium studies, NMR can be used in the classical way by recording spectra at different time intervals and measure the change in concentration. Small rate constants of 10^{-2}-10^{-4} s^{-1} can be measured by this method. However, the most common use of NMR is to study dynamic processes of systems in equilibrium. As mentioned, the NMR peaks are usually rather narrow. The NMR line widths, $\Delta\nu_{1/2}$ in the absence of exchange are given in equation 2.15.

$$\Delta\nu_{1/2} = 1/(\pi T_2^*) \qquad (2.15)$$

where T_2^* is the spin-spin relaxation time, which includes the effect of the inhomogeneity of the magnetic filed. T_2^* is also called the *transverse* relaxation time. Additional broadening can occur when there are exchanging species in the solution. Rate constant between 1 to 10^{10} s^{-1} can be studied depending on the chemical shift difference between the exchanging species and the natural transverse relaxation rate of the studied nucleus. When there is exchange between two species, two extreme cases may be distinguished. If the rate is much slower compared to the difference between the chemical shift of the individual species, two separate narrow peaks, one for each site, can be observed. Alternatively, if the exchange is much faster than the shift difference, the spectrum shows one narrow average peak for both exchanging sites. In between, there is a broadening of the individual peaks, which at certain point coalescence and give a common broad peak. The peak becomes narrower at increasing rate of exchange as illustrated in Figure 2.2. If the rate is in the slow exchange region, but fast enough to give a broadening of the individual lines, the measured line widths for each of the signals can be written as

$$\Delta\nu_{1/2} = 1/(\pi T_2^{\exp}) \qquad (2.16)$$

where $\Delta\nu_{1/2}$ is the measured line with at half height of the Lorenzian shaped peak and $T_2^{\exp}$ is the sum of contributions from *transverse* relaxation time, the inhomogeneity of the magnetic field, and the chemical exchange. The measured line widths of the *i*th species exchanging with *n* other species, can be written as

$$\pi\Delta\nu_{1/2}(i) = \pi\Delta\nu^{0}{}_{1/2}(i) + \sum_{j=1}^{n} k_{i,j} \qquad (2.17)$$

where $\Delta\nu^{0}{}_{1/2}(i)$ is the non exchange line width for the *i*th species and k_{ij} is the pseudo first order rate constant for the chemical exchange process from the *i*th to the *ij*th site.

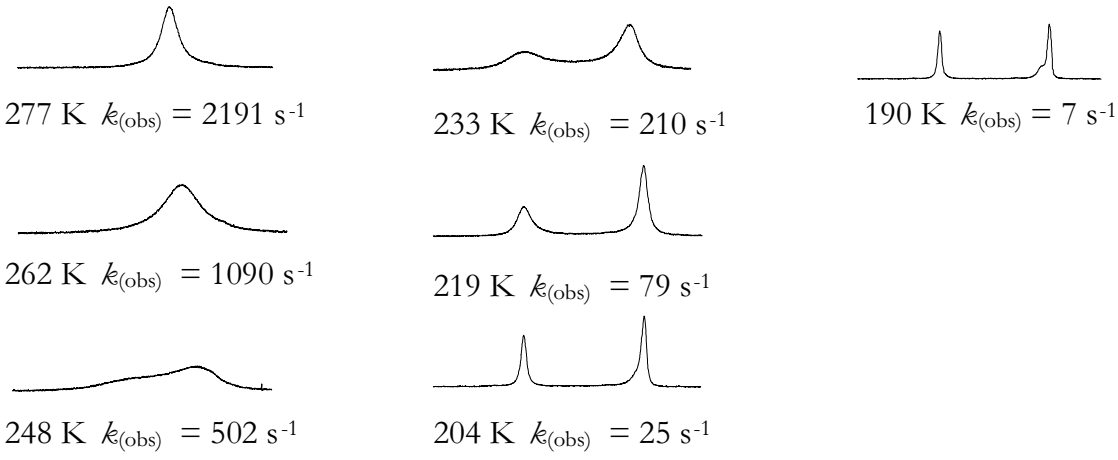

***Figure 2.2**. ^{1}H NMR spectrum of $UO_2(pic)_2F^-$ at different temperatures, only one part of the spectrum is shown. This illustrates the isomerisation reaction described in section 5.3.5.*

In systems where the chemical exchange is too slow to affect the line shape, but of the same order as the *longitudinal* relaxation rate ($1/T_1$), it is possible to evaluate the rate constants between two or more exchanging sites by so called magnetisation transfer experiment. Rate constants in the order of 10^{-2} to 10^{3} s^{-1} may be determined depending on the nucleus and magnetic field. Considering a two-site exchange between sites A and B; when a selective inversion (180° π_{sel} pulse) is applied to the signal A (or B), we will have the situation described in Figure 2.3. Depending on the time A are in excited state, there can be an exchange reaction between A and B transferring the negative magnetisation, or it may relax to its ground state before any exchange take place. After a period τ, a non-selective reading pulse (90°, $\pi/2$) generates observable peaks of the inverted and non-inverted signals. By varying the delay period τ, one can measure the rate of magnetisation transfer and from this the rate of exchange. At a small value of τ compared with the rate of exchange (k_A) and relaxation rate R_{1A}, there will be no time for the negative magnetisation to be transferred from A to B, and A has neither had time to relax.

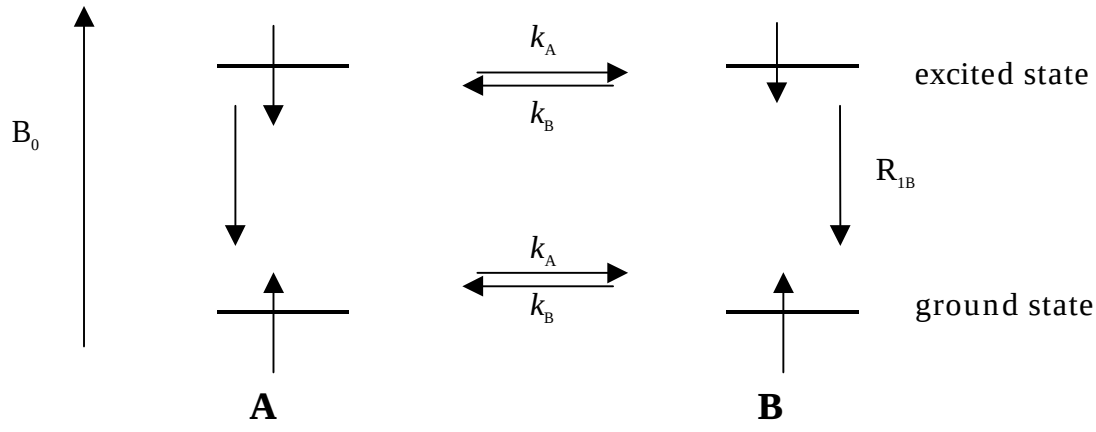

Figure 2.3. *Illustration of the principals of magnetisation transfer.*

At small τ, the observed spectrum will consist of a negative signal of A and a positive of B. When the period τ is increased, the net intensity will increase or decrease for the inverted and non-inverted signal, respectively as a result of exchange. When τ is long enough, the system has had time to equilibrate and all the signals are at their original intensity. An example of an inversion transfer experiment is given in Figure 2.4.

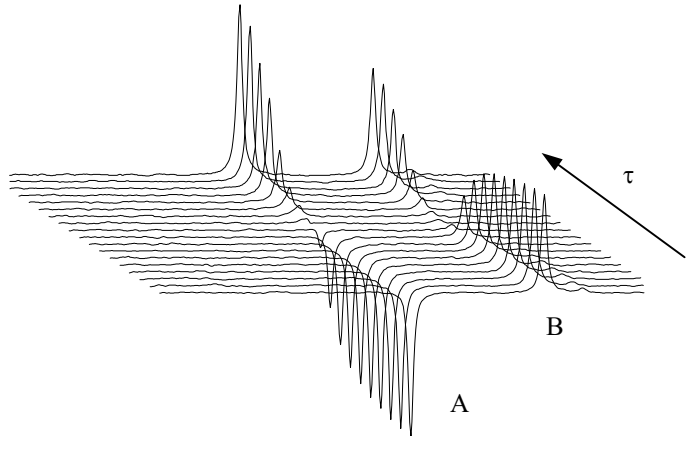

Figure 2.4. *^{13}C NMR, inversion transfer experiment of a solution of $UO_2(ox)F_3^{3-}$ and free oxalate, the peak from the complex is inverted.*

From the time dependence of the intensities, the rate constants can be calculated on the basis of the Bloch-McConnel equations modified for the transfer of magnetisation by chemical exchange, equation 2.18, generalist to an *i* number of sites and not only two sites as described above.

$$d[M_{i(t)}-M_{i(\infty)}]dt^{-1} = R[M_{i(t)}-M_{i(\infty)}] \qquad (2.18)$$

where $M_{i(t)}$ is the *z*-magnetisation of *i*th site at time *t*, $M_{i(\infty)}$is the equilibrium magnetisation and R is the so called rate matrix ($R = X\Lambda X^{-1}$ where X is the eigenvector matrix and Λ is the diagonal eigenvector matrix). The solution of the equation 2.18 can be written as:

$$M_{i(t)} = M_{i(\infty)} + \sum_{j=1}^{n} c_{ij} \exp(-\lambda_j t) \qquad (2.19)$$

where C_{ij} is:

$$c_{ij} = X_{ij} \sum_{k=1}^{n} (X^{-1})_{jk} [M_{k(0)} - M_{k(\infty)}] \qquad (2.20)$$

and λ_j are elements of Λ and $M_{i(0)}$ is the initial magnetisation of site *i*. The rate parameters can then be obtained by using a non-linear fitting procedure.

2.3 Methods for studying structures

Single crystal X-ray diffraction is the most precise and most used technique to determine structures in the solid state. The explosive development of computers and the invention of area detectors have made this a relative fast analytical tool when good single crystals are available. The preparation of suitable crystals is probably the rate determining step in the process. Nevertheless, there are many structures that cannot be solved by routine methods and require a deeper understanding of the X-ray technique to be solved. X-ray structure determination consists of three steps: produce and select a good crystal, measure the diffracted X-ray data and finally reduce and refine the obtained data. Growing crystals can be viewed upon more as an art than as a science, and there are few direct recipes on how to have success. A satisfactory crystal must possess uniform internal structure and be of proper size and shape. Generally, the preferred linear dimensions are 0.1-0.3 mm. Diffraction is a result of a periodic electron density in the crystal, and the crystals diffract light of wavelengths of same order as the interatomic distances. Since these distances are from one to a few ångstrøm, the diffraction is observed in the X-ray region (10^{-10} m). The angles of the scattered reflections contain information about the cell dimensions and the intensities give information of the atomic positions in the unit cell. The intensity of the scattering depends on the atomic number of the scattering atoms and

increases with increasing electron density. It can therefore be difficult to locate light atoms in the presence of heavy ones. The intensity is also dependent on the absorption of the X-ray in the crystal, and absorption generally increases with increasing number of heavy atoms. The sum of the contributions from all the atoms in the unit cell to the X-ray scattering is called structure factor (F_{hkl}), and its absolute value $|F_{obs,\mathrm{hkl}}|$ can be calculated from the measured intensities (I) of the X-ray reflections. This requires that they are corrected for several physical factors, Lorentz (L) and polarisation (p) factors as well as absorption and extinction if needed. The absolute value of the structure factor is given by equation 2.21.

$$\left|F_{hkl}\right| = \sqrt{\frac{KI_{hkl}}{Lp}} \qquad \text{where } p = \frac{1+cos^2\theta}{2} \tag{2.21}$$

K is a constant depending on the crystal size, beam intensity and a number of fundamental constants. It is usually omitted from the data reduction and a relative value of the structure factor is used. For a periodic structure, the electron density (ρ) is given by equation 2.22.

$$\rho(x,y,z) = \frac{1}{V}\sum_h\sum_k\sum F_{hkl}e^{-2\pi i(hx+ky+lz)} \tag{2.22}$$

When one knows the structure factor, it is a simple task to calculate the electron density. However, experimentally one obtains the absolute value of F_{hkl} making the task more difficult. There are two ways of solving this so called phase problem, either by statistical (direct) or heavy atom (Patterson) methods. By using the Patterson method, the heavy atoms in the structure are located. The known positions of the heavy atoms, uranium in our case, are then used to calculate the phase angle (δ):

$$F_{hkl} = \sum f_j e^{i\delta_j} \qquad \text{and} \qquad \delta = 2\pi(hx+ky+lz) \tag{2.23}$$

where f_{j} is the scattering factor. When the cell is centrosymmetric, as in the structure we determine, the phase angle is either 0° or 180°; hence, F_{hkl} is simply assigned a plus or minus sign. Using direct method to determine the phase angle, statistical

connections between the intensities of certain classes of reflections are used. Only a limited number of reflections are phased and Fourier summation is used to determine the atoms approximate positions. The known atom positions are used to obtain a more correct phase angle which in turn produce a more detailed electron density map. When the structure is known the theoretical F_{hkl} can be calculated. These values are compared with the experimental $|F_{hkl}|$. The atom positions and their thermal parameters are refined using a least square method, minimising the function 2.24.

$$R = \frac{\sum \left| |F_{obs,hkl}| - |F_{hkl}| \right|}{\sum |F_{obs,hkl}|} \qquad (2.24)$$

The value of R indicates how good the fit is between the structure model and the experimental data. This value is widely used as a guide of the correctness of the model. The short summary presented here is of course a very simplified description of the technique, and the reader is referred to the literature on this topic to obtain more detailed information [22].

It is more difficult to obtain exact structural data in solution. Extended X-ray Absorption Fine Structure (EXAFS) and Large Angle X-ray Scattering (LAXS) can be used to obtain bond distances and to some extent coordination numbers. A combination of several NMR techniques may also be used for structure analysis. From the chemical shift and coupling pattern of a compound, structural information can immediately be obtained. The coupling pattern contains information about neighbouring atoms and, hence, the location of ligands in the complexes can be revealed. The number of equivalent sites contains information about the symmetry of the molecule. The molecular geometry may be deduced by the known symmetry and stoichiometry of the complex. For organic compounds, both one and two-dimensional ^{1}H and ^{13}C NMR techniques are used as standard routines to determine structures. Inorganic compounds rarely exist as a single complex in solution. This can make structural analysis more complicated due to fast reactions between the species that result in overlapping peaks. The solvent molecules are usually involved in coordination and can complicate the interpretation of the spectra even more. Sometimes the resolution might be improved by introducing a shift reagent. Such a

reagent modifies the local field, and it can result in either an increase of the spectra window or an increase in the shift differences between the species.

III Coordination Chemistry

3.1 General background.

At the end of last, and at the beginning of this century, Alfred Werner made his pioneering work on the coordination theory. His work formed the platform of modern coordination chemistry [23]. Metal complexes, at least the *d*-transition elements, are sometimes even called Werner complexes. Werner's theory was based on studies performed on the transition elements, mainly Co(III) and Cr(III). Later, the coordination theory was extended by Lewis, Langmuir and Sidgewick to describe the chemical bonding in coordination compounds. Today, a much more detailed understanding of the properties of the coordination bond may be obtained through various quantum chemical methods [24].

A metal ion is always attached to ligands, either in form of solvent molecules or any other Lewis bases present. The ligands can be anionic as deprotonated acids (*e.g.* F^-, OH^-, RCO_2^-) or uncharged, but with one or more lone pairs of electrons (*e.g.* H_2O, NH_3, CO). Ligands that contain several potential donor atoms have a possibility to be chelating. Both chelating ligands and atoms with two or more free lone pairs of electrons can also act as bridging ligands and form polynuclear species. Metal complexes form a variety of isomers. The concept of isomers and isomerism was already used by Werner and formed the basis for his theory and the deduction of the coordination geometry of the complexes studied. Werner studied inert complexes, which made it possible to isolate the different isomers and analyse them separately. Today, modern techniques make it possible to identify isomers in fast dynamic equilibrium, where isolation is not feasible.

The number of ligands that can be coordinated and the geometry of the coordination shells are dependent on the size and charge of the metal ion and on the structure and charge of the ligands. High charge on the metal ion and small ligand size or/and charge usually favour high coordination numbers, and vice versa. There is an upper limit, for steric reasons, of the number of ligands that can coordinate to a particular metal ion. High coordination numbers are only feasible for large central ions and multidentate ligands with a short distance between the donor atoms, *e*.g. NO_3^- and CO_3^{2-}. The lanthanides and actinides are large and can therefore have large

coordination numbers. Since the actinides in oxidation state III, IV and VI are studied in this work, a description of their general properties will be described in the next two sections.

3.2. Coordination properties of uranium(VI)

The linear dioxouranium(VI) has a special coordination geometry where all the coordination sites are situated in the equatorial plane surrounding the central atom. Five coordination, in type of a pentagonal bipyramid structure, is the most common geometry, but there are also examples of four and six donor atoms in the equatorial coordination plane. Octahedral type of coordination occurs when the ligands are large and bulky as in $[UO_2Cl_4](Et_4N)_2$ [25] and $UO_2(HMPA)_4$ [26]. There are many examples of pentagonal bipyramidal structure of type UO_2L_5 both in solution and solids, *e.g.* $UO_2(H_2O)_5^{2+}$ [27] and $K_3UO_2F_5$ [28]. Hexagonal coordination of type UO_2L_6 is not known. Nevertheless, there are many examples of six-coordination with bidentate ligands. These ligands may either form penta- or hexagonal structures depending on distance between the coordinated donor atoms, the ligand "bite". Chelates with bites in the range of 2.5-2.8 Å fit with five coordination [29], usually by forming five membered rings. Bidentate ligands of smaller bites ~2.2 Å, may accommodate six donor atoms around uranyl, as *e.g.* $UO_2(CO_3)_3^{4-}$ [30] and $UO_2(acetate)_3^-$ [31]. The complexes are hexagonal bipyramids both in solid state and solution. Uranyl-oxalate serves as a good illustration on the possibility to have both five and six coordination [29].

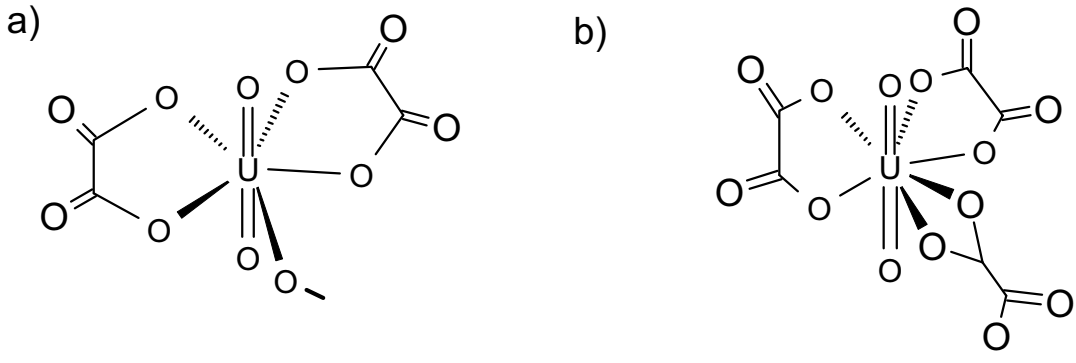

Figure 3.1*. Structure of a) $[UO_2(ox)_2]_n^{2n-}$ [32] O- donates part of the chain forming oxalate group, b) $[UO_2(ox)_3]^{4-}$ [33].*

In the polymeric structure of $(NH_4)_2(UO_2)(ox)_2$ [32], one of the oxalate groups is bonded in bidentate fashion to one uranyl, and the other is bonded as a bidentate to one uranium and unidentate to another forming a chain, Figure 3.1a In the monomeric $(NH_4)_4(UO_2)(ox)_3$ two oxalate ligands are bidentate and one is unidentate coordinated [33], Figure 3.1b. The O-O distance of the oxalate for the 1,4 and 1,3 bonds are 2.54 Å and 2.21 Å, respectively.

The -yl oxygens are kinetically inert, except when excited by UV light. The mean U-O_{yl} distance from 180 different crystal structures [34] is 1.77 Å, ranging from the shortest distance of 1.5 Å to the longest at 2.08 Å. The bond length is correlated with the basicity of the equatorial ligands, where the longest bonds are found for oxide ions and the shortest for anions of strong acids such as nitrate. With a few exceptions, the deviation from linearity is less than 5^{O}. The bond distances in the equatorial plane vary with the size and nucleophilic properties of the ligands and the number of secondary interaction with neighbouring atoms in the structure. Fluoride is one of the strongest bonding ligands and the average bond distance in $K_3UO_2F_5$ [28] is 2.24 Å. Oxygen has different coordination modes, and the distance to uranium is depending on whether it is part of a hydroxide (2.2-2.4 Å [35]), carbonate (2.4-2.6 Å [30]), or a chelating or non chelating carboxylate group (2.43(1) Å and 2.57(2) Å for oxalate bonded 1,3 and 1,4 respectively [33]). Nitrogen is usually a weaker electron donor and has a longer bond distance to uranium than oxygen, as illustrated in complexes where both nitrogen and oxygen are present in forms of chelating ligands. In uranyl-dipicolinate the average bond distances are 2.61 Å and 2.39 Å for U-N and U-O, respectively [36]. In uranyl-pyrazinate the U-N bond is 2.58 Å and U-O is 2.32 Å [37], and for uranyl monopicolinate the U-N bond is 2.58 Å and U-O 2.34 Å [38].

3.3. Coordination chemistry of tetra- and trivalent actinides

Tetravalent (M^{4+}) and trivalent actinides (M^{3+}) have more varied coordination geometry than the “yl”-ions, MO_2^{+} and MO_2^{2+} [24]. Trivalent actinides similar properties as the lanthanides(III) which normally are eight- or nine coordinated, but six and seven coordination are also known. The geometry for the nine-coordinated complexes is usually a tricapped trigonal prism or the less symmetrical monocapped square antiprism; these geometries are often slightly distorted. Tetravalent actinides

are more studied than the trivalent, because they are usually more stable and therefore easier to handle experimentally. Eight coordination is most common, but there are examples of coordination number from 4 up to 14 [24]. The most common geometries for eight coordinated lanthanides are square antiprism and dodecahedron. A less frequent structure is a bicapped trigonal prism. Most of the structures are distorted from these idealised categories making it difficult to distinguish between for example a distorted dodecahedron and a distorted square antiprism.

3.4 Structure analysis of ternary uranyl complexes.

The crystal structure of $Na_2UO_2(pic)F_3*4H_2O$ was determined. Figure 3.2 depicts the complex from two different orientations to show the coordination geometry around uranium.

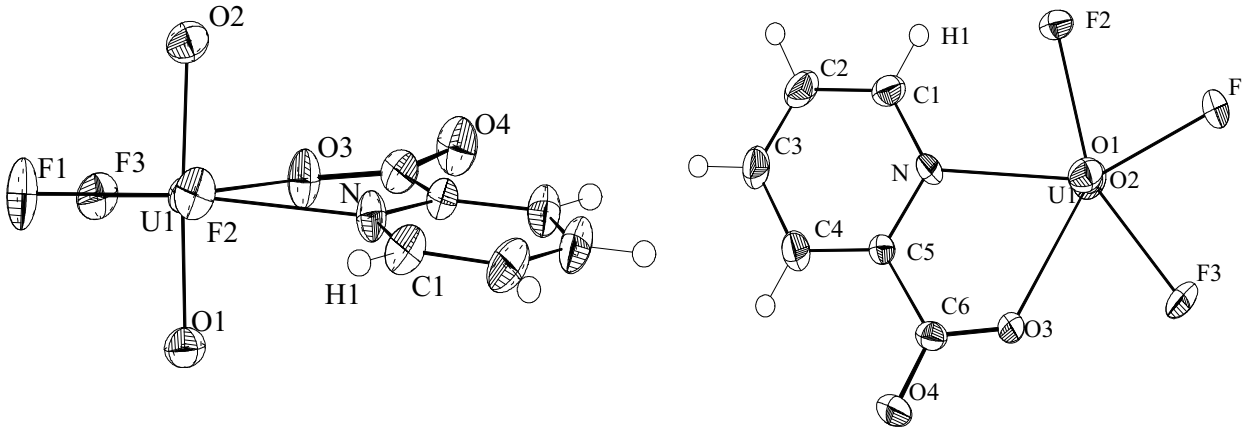

***Figure 3.2**. Molecular structure of $[UO_2(pic)F_3]^{2-}$, the atoms represented with 50% probability ellipsoids.*

The complex has a distorted pentagonal bipyramid structure. The picolinate ligand is slightly tilted out of the equatorial plane. This is probably a result of a repulsion between the F2 fluoride and the hydrogen on C1; the distance between these two atoms is 2.34 Å. One might believe that the F-H interaction is a result of hydrogen bonding rather than a repulsive force, but the distance between them is too long for bonding. In addition, the tilting indicates an absence of attractive forces

since it results in a longer F-H distance. The U-F (2.24 Å) and U-N (2.60 Å) distances are in good agreement with the bond distances found in the literature. It is interesting to note that the U-O3 bond distance increased from 2.34(1) Å in the binary uranyl-picolinate [38] complex to 2.447(4) Å for this ternary complex. This difference might be due to a negative charge effect from the fluorides.

The unit cell contains two formula units. The organic ligands are pointing towards each other and are stacked as shown in Figure 3.3 with a distance of 3.6 Å. The same packing is seen in the corresponding oxalate compound, $Na_3[UO_2(ox)F_3]*8H_2O$ [39]. Figure 3.3 clearly shows how the sodium atoms are interconnected building a chain where also coordinated fluorides and "yl" oxygens are included. The coordination geometry around the sodium atoms is distorted octahedral.

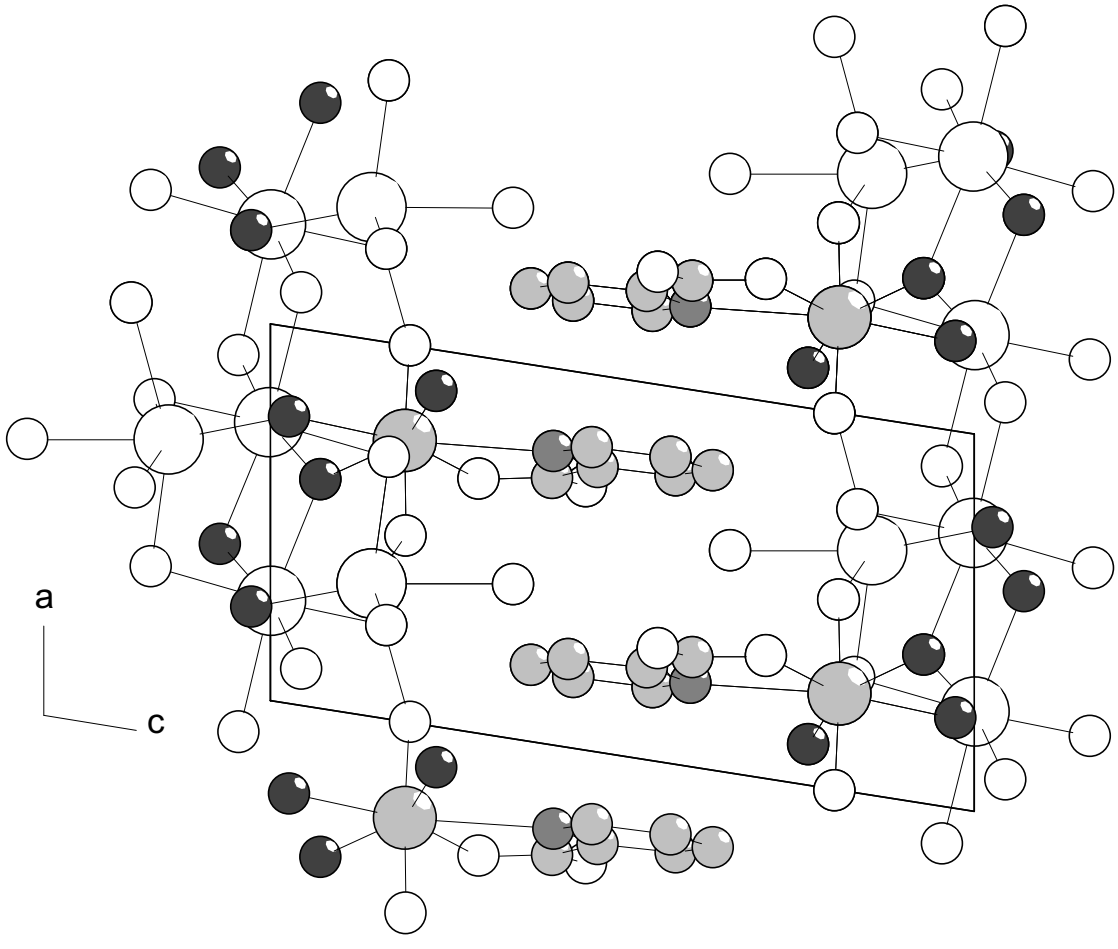

***Figure 3.3**. Packing structure of $Na_2UO_2(pic)F_3*4H_2O$ viewed down the b-axis. Sodium and oxygen atoms are white, uranium and carbon are light grey, nitrogen is grey and fluoride is dark grey.*

The coordination of ternary uranyl complexes in solution was mainly studied using NMR spectroscopy. By ^{19}F-NMR, it was possible to observe separate peaks for all the complexes that are formed. In several cases even the different fluorides within the complex could be distinguished, for example in $UO_2(ox)F_3^{3-}$. The spectrum of this complex is shown in Figure 3.4.

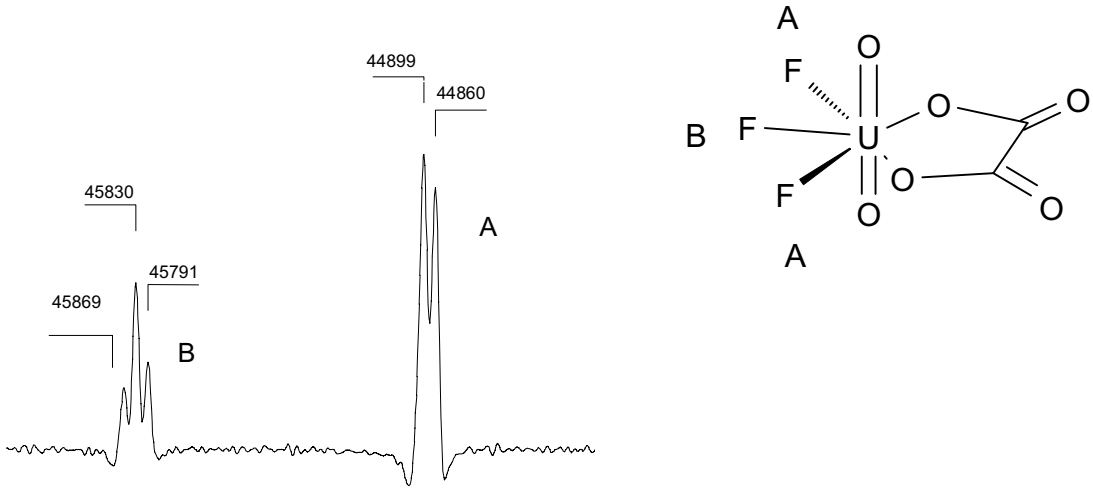

Figure 3.4 *^{19}F NMR spectrum of $UO_2(ox)F_3^{3-}$ at –5^{O}C.*

The relative intensity between B and A is 1:2. B couples with two fluorides (A) and giving rise to a triplet, while A is coupled to only one fluoride (B) resulting in a doublet. The only explanation for this observation is a complex with pentagonal coordination geometry, since the symmetry plane makes the two edge fluorides equivalent. An addition of one water molecule would result in a hexagonal coordination plane, and all the fluorides would then have been magnetically different. The same 1:2 ratio was observed in the $UO_2(acetate)F_3^{2-}$ complex, even though the peaks were broader due to faster exchange. This is evidence for a bidentate coordination mode of acetate. Acetate is a weak ligand, and knowing the magnitude of the formation constant alone is not sufficient to determine whether acetate is uni- or bidentate.

Picolinate is an asymmetric ligand, and the three fluorides in $UO_2(pic)F_3^{2-}$ are chemically different and give rise to three separate fluoride peaks. The middle fluoride splits up into a triplet due to the coupling with the two edge fluorides, which on the other hand are too broad to show any coupling due to fast exchange

reactions. The fluoride spectrum of $UO_2(pic)F_3^{2}$ is shown in chapter 5, Figure 5.5. An interesting observation is that one of the edge fluorides is shifted to much lower field than the other two. The ^{1}H-NMR spectrum of the same compound shows four proton peaks corresponding to the picolinate protons, where one of them is shifted about 2 ppm higher than the other three. These two observations can be explained in accordance to the crystal structure shown in Figure 3.2, and indicates a clear repulsive interaction between F2 and H1.

It has also been possible to identify different isomers in many of the studied ternary complexes. In non-saturated complexes of type $UO_2LF_2(H_2O)$ and $UO_2LF(H_2O)_2$, there are several possible isomers. As an example, $UO_2(ox)F_2(H_2O)^{2-}$ gives rise to three peaks in the ^{19}F-NMR spectrum. Considering a pentagonal coordination symmetry around uranyl, there are two possible isomers for this complex shown in Figure 3.5, and consequently three magnetically different fluorides

Figure 3.5 *The two possible isomers for $UO_2(ox)F_2(H_2O)^{2-}$.*

There are three possible isomers for the saturated complex $UO_2(pic)_2F^{-}$, as shown in Figure 3.6.

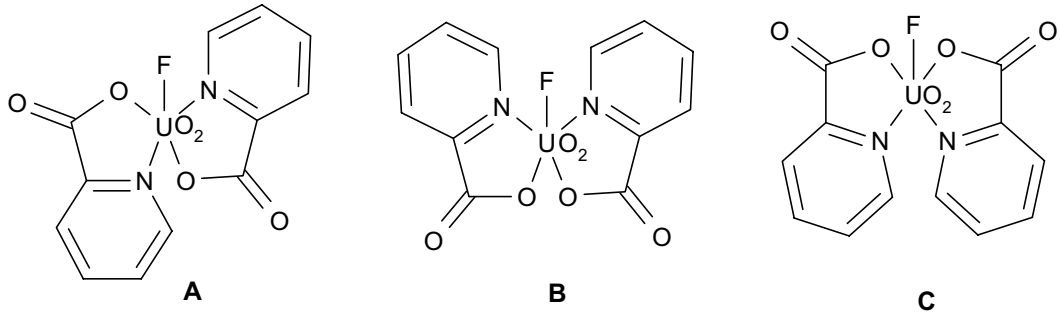

Figure 3.6 *The three possible isomers of $UO_2(pic)_2F^{-}$*

The isomerisation reaction between the complexes is slow in methanol at –54 °C. Two isomers have been identified using ^{1}H-NMR. The most stable one is designated A. The crystal structure of the binary $UO_2(pic)_2(H_2O)$ [38] also shows a *trans* coordination of the two picolinate ligands. The *trans* geometry is probably the most stable isomer for steric reasons. B is assumed to be the minor isomer, while the C isomer is not observed, probably because it is less stable than the two others since all the negative groups are adjacent to each other, resulting in an uneven charge distribution.

IV Equilibrium Studies

4.1 General background

The concept of equilibrium constants was first elaborated in 1864 by Gullberg and Waage when they formulated the law of mass action. Van't Hoff further completed the picture of the dynamic equilibrium process and formulated the equilibrium expression we know today. The formation of the complex ion ML and its equilibrium constant (K) is expressed by the following equation:

$$M + L \underset{k_{-1}}{\overset{k_1}{\rightleftharpoons}} ML, \qquad K = \frac{[ML]}{[M][L]} \tag{4.1}$$

The equilibrium constant is simplified using the ratio of concentrations and not activities. This is only valid at zero ionic strength, which is never the working medium in equilibrium studies. A more thorough discussion of this problem and the different techniques to quantify equilibrium constants is found in chapter 2.

Equilibrium is a dynamic process where the forward and reverse reaction rates are equal. Assuming that reaction (4.1) is an elementary reaction, we have the simple relation

$$\frac{d[ML]}{dt} = k_1[M][L] - k_{-1}[ML]; \quad \frac{d[ML]}{dt} = 0 \text{ at equilibrium, it follows that}$$

$$k_1[M][L] = k_{-1}[ML] \quad \Rightarrow \quad K = \frac{k_1}{k_{-1}} \tag{4.2}$$

where k_1 and k_{-1} are the forward and reverse rate constants, respectively. The equilibrium constants can be calculated if the rate constants are determined. It is important that the reaction is elementary; otherwise, the equilibrium constant is not the ratio between two rate constants. An equilibrium expression is an equation for the total reaction, which in turn may consist of several elementary reactions. The rate equation will be a function of all the steps in the reaction sequence. Dynamic processes will be discussed in more detail in chapter 5.

The magnitude of the equilibrium constants reflects the stability of the complexes depending on the nature of both the ligand and the metal ion. The concept

of hard- and softness has been utilised to describe the metal and ligand properties. The classification of the periodic elements into these two groups was first made by Ahrland et al. in 1958 [40]. Hardness is characterised by high electronegativity and low polarisability (e.g. F^- and Al^{3+}) while the reverse is true for the soft acids and bases (e.g. $Ag^+$and I^-). Hard acids bind strongly to hard bases and soft acids to soft bases. The concept of hard / softness makes it feasible to compare and summarise a vast number of equilibrium data to predict unknown equilibrium constants. Ever since Niels and Jannik Bjerrums work, the coordination chemists have been interested to find a way to describe and compare the size of the stepwise equilibrium constants between several binary systems. If the same donor atom contributes in all these reactions, the stepwise equilibrium constant should not be influenced by this, unless the size of the ligand causes steric hindrance. Three main factors contribute to the magnitude of the stepwise constant:

Statistical factors, which are decided by the coordination geometry and the number of free sites for coordination of ligands. The statistical factor can be calculated for central ions and ligands with known coordination geometry. For a unidentate ligand in a system with a maximum of N coordination sites and n coordinated ligands, the statistical factor is

$$\frac{K_n}{K_{n+1}} = \frac{(N - n + 1)(n + 1)}{n(N - n)} \qquad (4.3)$$

For multi-dentate ligands, the relation between the stepwise formation constant will be different. In this case, one needs to consider whether all combinations of coordination sites are feasible, or not. Bidentate ligands can for example in an octahedral complex only bind in a cis coordination mode

2. Electrostatic factors may also contribute to the size of the stepwise equilibrium constant. The strength of bonding is related to the product of the charges of complex and ligand. This is certainly less important when the bonds are of more covalent nature. The theory of electrostatic effect is simplified by using the total charge of complex and ligand. Our studies indicate that this is a wrong picture, it is the local charge, which seems to be of main importance.

3. Geometrical factors should also influence the size of the constants. Repulsion

between the ligands will *e.g.* decrease the stability of complexes. This is of course most important when increasing number of coordinated ligands.

Increased stability arises when the ligands can form chelating complexes, especially when there are 4-6 atoms in the chelate ring. The effect is usually due to a favourable entropy change associated with ring formation. Details of the different effects described above can be read in work by J. Bjerrum [41] and Grenthe et al. [42].

4.2 Thermodynamic properties of the actinides

The actinides are hard acids and, hence, bind strongly to hard bases such as carbonate, hydroxide and fluoride. The hardness decreases in the order $M^{4+} > MO_2^{2+} > M^{3+} > MO_2^{+}$, which can be illustrated by the formation constant of fluoride complexes. Their order of magnitude are 10^8, 10^4, 10^3 and 10 for M = Th^{4+}, UO_2^{2+}, Cm^{3+} and NpO_2^{+}, respectively [43].

The most studied actinide is uranium(VI). Extensive thermodynamic studies have been undertaken, especially on binary complexes, which have been reviewed by Grenthe et al. [4]. The hydroxide complexes are important in a broad pH range starting at around pH 3. OH^- is a good bridging ligand; hence, the hydrolysis of UO_2^{2+} results almost exclusively in polynuclear species even in very dilute solutions. Predominant species are $(UO_2)_2(OH)_2^{2+}$ and $(UO_2)_3(OH)_5^{+}$, the latter at higher pH. Since hydroxide is such a strong ligand, it is important in coordination chemistry studies, always to consider whether binary uranyl-hydroxide complexes or mixed U(VI)-OH-L complexes may be formed.

Carbonate is another good bridging ligand. The stable tris-carbonate complex $(UO_2)_3(CO_3)_6^{6-}$ is formed at a low carbonate concentration. When the carbonate concentration is increased, the monomer $UO_2(CO_3)_3^{4-}$ complex is predominant.

Fluoride has similar properties to hydroxide, being of almost equal size and hardness. Even so, it is a poor bridging ligand in solution where it only forms monomer complexes with uranium(VI). However, fluoride is well known to be bridging in solid state [44]. The other halides have much less affinity for the uranyl ion. Carboxylate ligands form weaker complexes than carbonate. The affinity in general increases with the basicity of the ligand [45]. Strong complexes can be formed when the ligand contains several carboxylate groups that can form chelates, such as

for example oxalate. Uranyl has a fairly small affinity for nitrogen donors, which might be counter intuitive since nitrogen is a rather hard donor. However, there are relatively few studies performed with nitrogen donors due to experimental difficulties. Aliphatic nitrogen is a strong Brønsted base and they generally deprotonate water to form OH^-. The stable uranyl-hydroxide complexes are therefore formed instead of possible amino complexes. The hydroxide problem can be reduced by including the aliphatic nitrogen in a polydentate ligand, as for example in the EDTA complex. Aromatic nitrogen is a weaker Brønsted base; thus, complex formation reaction can be studied without problems of hydrolysis. However, aromatic nitrogen is also a weaker Lewis base and has small affinity to uranyl. The affinity will increase dramatically if it can form chelates. Picolinate ligand serves as an excellent example. To conclude, the apparent small affinity between actinides and nitrogen donors is to large extent a result of the high basicity of nitrogen, which results in the formation of sufficiently large amount of hydroxide that effectively competes with the weaker N-donors.

For comparison, the stability of uranyl complexes with some of the most typical inorganic and organic ligands are listed in Table 4.1

Table 4.1. *Formation constants of UO_2L at I = 0 M and 25^{O}C [4].*

	OH^-	F^-	Cl^-	CO_3^{2-}	SO_4^{2-}	NO_3^{2-}	PO_4^{3-}	ac	ox	pic
logβ	8.8	5.09	0.17	9.68	3.15	0.30	12.23	2.42[f]	5.99[g]	4.48[h]

[f] I = 1 M 20^{O}C [46], [g] I = 1 M [47], [h] I = 1M this work

In contrast to the extensive thermodynamic studies done on binary uranyl systems, little is known about ternary uranyl complexes in aquatic environment. This is due to experimental difficulties. Using potentiometry to study ternary systems, it can be difficult to interpret the results when only -log[H^+] is measured. When an additional ion selective electrode or a spectroscopic technique like NMR, can be utilised, the task becomes more feasible. Previous studies of ternary systems refer mainly to complexes containing hydroxide and one additional ligand such as carbonate [48] or sulphate [49]. Examples also exist of studies undertaken on mixed

complexes with different carboxylic acids using ligands with a rather large range of formation constants [50].

4.3 Experimental approach and equilibrium results of the $UO_2L_pF_q$ complexes

The equilibria of the ternary complexes were studied using both potentiometry and NMR spectroscopy. For quantifying the equilibrium constants, the titration results have in most cases been preferred, since this method has a high inherent precision. The total reaction for the complex formation reaction in our ternary system is:

$$UO_2^{2+} + pL + qF^- \rightleftarrows UO_2L_pF_q \qquad (4.4)$$

where L is carbonate, oxalate, picolinate or acetate. With this choice of components, the formation constant will be:

$$\log\beta_{pq} = \frac{[UO_2L_pF_q]}{[UO_2^{2+}][L]^p[F^-]^q} \qquad (4.5)$$

To make it easier to interpret the experimental results, we have chosen to keep either the total concentration of L or F constant in the titrations; the choice depends on the system in question. The total uranyl concentration was also kept constant throughout the titrations. Both the free fluoride and, indirectly, the free L concentration were measured throughout the experiment using an ion selective fluoride electrode and a quinhydrone electrode, respectively. When the ligand is oxalate or acetate, the total concentrations of L and F^- were selected in such a way that the conditional equilibrium constants defined by equation (4.6) could be determined. In the picolinate and carbonate systems, the total fluoride concentrations were constant and the conditional constants defined in equation (4.7) could be determined.

$$UO_2L_p + qF^- \rightleftarrows UO_2L_pF_q \qquad (4.6)$$

$$UO_2F_q^{2-q} + pL \rightleftarrows UO_2L_pF_q \qquad (4.7)$$

In reaction 4.6 the average number of fluoride ($\bar{n}_F$) that is bonded to uranyl was calculated, and the total fluoride concentration was used as the error carrying variable in the least square program LETAGROP [10].

$$\bar{n}_F = \frac{[F]_{tot} - [F] - [HF]}{[UO_2^{2+}]_{tot}} \qquad (4.8)$$

This approach is not satisfactory for reaction 4.7, because the total fluoride concentration is constant and the free fluoride concentration almost constant.

Instead, the number of L bonded to uranyl (4.9) was calculated using the total proton concentration as the error carrying variable in the least square refinements.

$$\bar{n}_L = \frac{[L]_{tot} - [L] - [HL]}{[UO_2^{2+}]_{tot}} = \frac{[L]_{tot} - (1 + \log\beta_{HL}[H^+])\dfrac{[H^+]_{tot} - [H^+]}{\log\beta_{HL}[H^+]}}{[UO_2^{2+}]_{tot}} \qquad (4.9)$$

For L = carbonate, carbonic acid (H_2L) is also encountered in the equation. As discussed in chapter 2, the uncertainty in the $\bar{n}$ function depends on the difference between the total and measured concentrations. When calculating $\bar{n}_F$ from equation 4.8, the uncertainty is largest at high free fluoride concentration due to the small difference between $[F^-]_{tot}$ and $[F^-]$. In equation 4.9, the largest uncertainty is at high [L], *i.e.* at high values of -log$[H^+]$.

Titration curves for the acetate and carbonate systems are plotted in Figure 4.1 as a representation of reaction 4.6 and 4.7, respectively. The species distribution in a typical titration is plotted next to the titration curves.

The equilibrium constants $\log\beta_{pq}$ for reaction 4.4 are summarised in Table 4.2. The uncertainties are equal to three times the estimated standard deviations. Almost all of the complexes have been identified by ^{19}F-NMR at –5^{O}C. The results obtained from these experiments are in agreement, within the experimental error, with the equilibrium constants derived by potentiometry. An exception is $\log\beta_{13}$ calculated for the acetate system. NMR and potentiometry experiments were in this case not in agreement. An equilibrium constant with a small standard deviation ($\log\beta_{13}$ = 11.13 ± 0.09) was determined from the potentiometric data. However, a maximum of 5 % of the total uranyl concentration was present as $UO_2(ac)F_3^{2-}$in these experiments. In the NMR studies we could work with much higher concentration of fluoride. From the integrals we determined that up to 60% of the uranyl concentration was present as $UO_2(ac)F_3^{2-}$, and the value $\log\beta_{13}$ = 11.7 ± 0.1 was obtained. This is significantly different from the value found from the potentiometric data. The NMR value is more accurate, even though not more precise, because of the high concentration of the complex. It is also more reasonable from a chemical point of view, since the stepwise formation constant for the acetate system should be similar to the other studied ligands. This serves as a good example of how important it is to be critical when

using least square refinements, and particular to use the precision in the equilibrium constant of a minor species, as an indication that the species is really present.

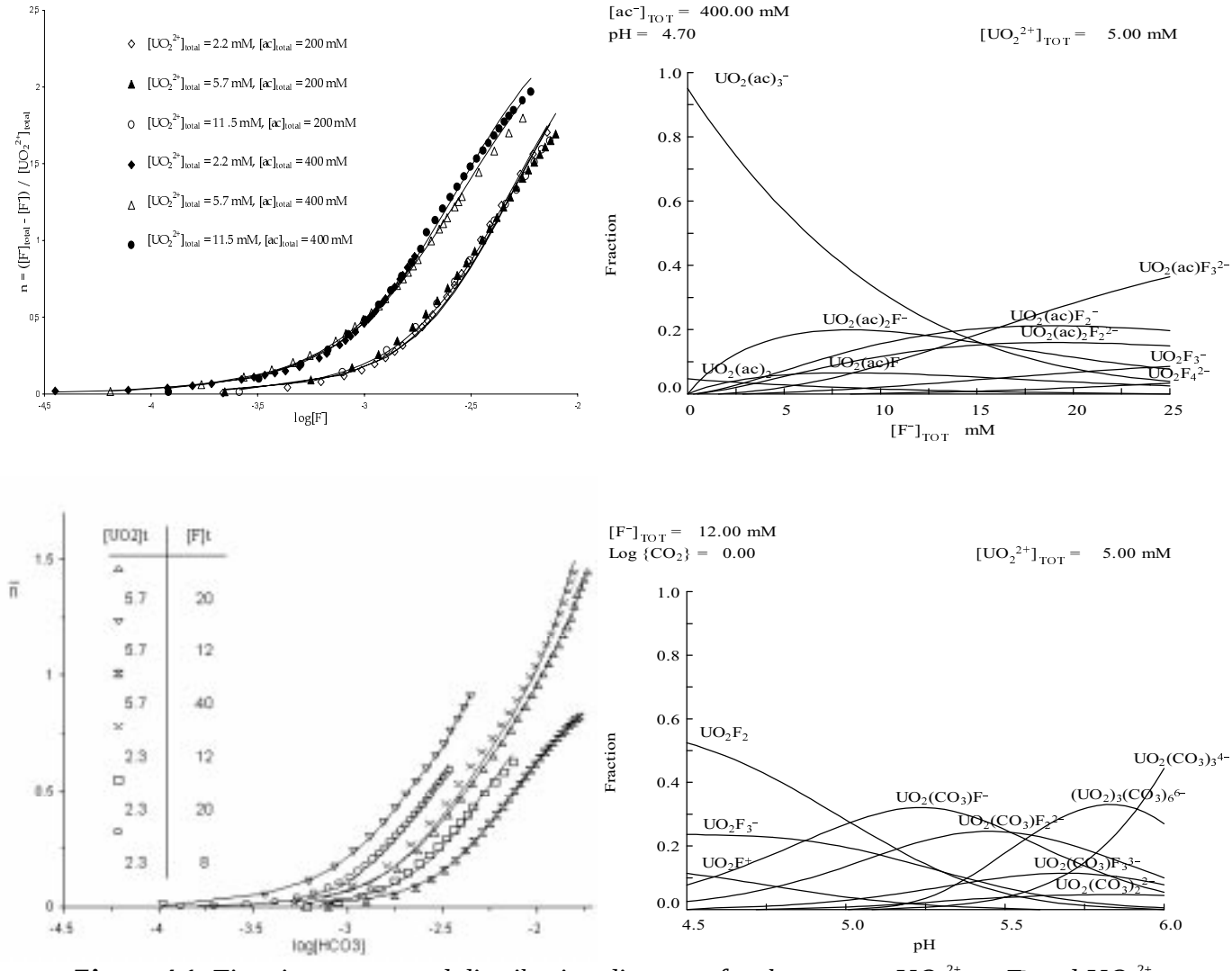

Figure 4.1*. Titration curves and distribution diagrams for the ternary UO_2^{2+}-ac-F^- and UO_2^{2+}-CO_3^{2}-F^- systems.*

In Table 4.3 and 4.4, the stepwise equilibrium constants are listed for addition of subsequent fluoride or acetate, respectively. The addition of fluoride to for example UO_2L, involves only three possible coordination sites, while the addition of fluoride to the uranyl aqua ion can take place at five coordination sites. To compare the stepwise constants in the binary, respectively ternary systems, it is necessary to correct for this statistical factor. The corrected values are given as italics in the tables.

Table 4.2. *Formation constants, log β_{pq}, for the reactions $UO_2^{2+} + pL + qF^- \rightleftarrows UO_2L_pF_q$ in 1.0 M $NaClO_4$ media at 25^{O}C. * Determined by ^{19}F NMR at –5^{O}C.*

L	UO_2LF	UO_2LF_2	UO_2LF_3	UO_2L_2F	UO_2L_2F
carbonate	12.56 ± 0.05	14.86 ± 0.08	16.77 ± 0.06		
oxalate	9.92 ± 0.06	12.47 ± 0.05	14.19 ± 0.05	13.86 ± 0.01	
picolinate	8.94 ± 0.01	12.28 ± 0.02	14.11 ± 0.06	12.33 ± 0.01	
acetate	6.66 ± 0.14	9.63 ± 0.04	11.70 ± 0.1*	7.65 ± 0.07	10.15 ± 0.08

Table 4.3*. The stepwise equilibrium constants, log K_{q+1}, for the reactions $UO_2F_q^{2-q} + F^- \rightleftarrows UO_2F_{q+1}^{1-q}$, q = 0 to 2. The constants in the binary system [51] are equal to 4.54, 3.44, and 2.43, respectively. The values in brackets are corrected for the statistical factor.*

L	$UO_2L + F^- \rightleftarrows UO_2LF$	$UO_2LF + F^- \rightleftarrows UO_2LF_2$	$UO_2LF_2 + F^- \rightleftarrows UO_2LF_3$	$UO_2L_2 + F^- \rightleftarrows UO_2L_2F$	$UO_2L_2F + F^- \rightleftarrows UO_2L_2F_2$
carbonate	4.08 (4.30)	2.30 (2.60)	1.91 (2.39)		
oxalate	3.93 (4.15)	2.55 (2.85)	1.72 (2.20)	3.32 (4.02)	
picolinate	4.46 (4.68)	3.34 (3.64)	1.83 (2.31)	4.16 (4.86)	
acetate	4.24 (4.46)	2.97 (3.27)	2.07 (2.55)	3.23 (3.93)	2.50 (3.10)

Table 4.4*. The stepwise equilibrium constants, log K_{p+1}, for the reactions $UO_2L_p + L^- \rightleftarrows UO_2L_{p+1}$, p = 0 to 1 or 2. The constants in the binary systems are equal to: 8.48, 7.16 and 6.2 for L = carbonate [4], 5.99, 4.55, and 0.46 for L = oxalate [47], 4.48 and 3.66 for L = picolinate, and 2.42, 2.00, and 1.98, for L = acetate [52]. The values in brackets are corrected for the statistical factor.*

L	$UO_2F + L^- \rightleftarrows UO_2LF$	$UO_2F_2 + L \rightleftarrows UO_2LF_2$	$UO_2F_3 + L \rightleftarrows UO_2LF_2$	$UO_2LF + L^- \rightleftarrows UO_2L_2F$	$UO_2LF_2 + L^- \rightleftarrows UO_2L_2F_2$
carbonate	8.02 (8.24)	6.88 (7.28)	6.36 (7.06)		
oxalate	5.38 (5.60)	4.49 (5.09)	3.78 (4.48)	3.94 (4.24)	
picolinate	4.40 (4.62)	4.30 (4.69)	3.70 (4.40)	3.39 (3.69)	
acetate	2.12 (2.34)	1.65 (2.04)	1.29 (1.99)	0.99 (1.29)	0.52 (0.82)

Before discussing the derived values, there are two observations that are of particular interest. In the carbonate system, we do not detect any coordination of a second carbonate in the ternary complexes. The most likely reason is that the formation of the binary complexes $UO_2(CO_3)_3^{4-}$ and $(UO_2)_3(CO_3)_6^{6-}$ are competing when the carbonate concentration is increased. This trend can be observed in the distribution curve in Figure 4.1. An additional complex is formed in the acetate system, $UO_2(ac)_2F_2^{2-}$. Acetate is a much weaker ligand than the other investigated ligands and the coordination may switch between bi- and unidentate. The low stepwise acetate constant for this complex may indicate a unidentate coordination. Another possibility is that, the complex may be six coordinated, a hexagonal bipyramidal coordination geometry is observed in the $UO_2(ac)_3^-$ complex [53].

The stepwise constants shown in Tables 4.3 and 4.4 are surprisingly high. Intuitively, a decrease in the formation constant is expected when other ligands already have been coordinated. With few exceptions, the stepwise constants for the binary and ternary systems are almost equal, at least when the statistical factor has been taken into account.

As described in chapter 3, $UO_2LF_2(H_2O)$, $UO_2LF(H_2O)_2$ and $UO_2(pic)_2F^-$ consist of different isomers. Using potentiometry in fast dynamic systems, it is not possible to distinguish between them. The constants in table 4.4 will therefore be an average of their individual formation constants.

4.4 Equilibrium data in the curium(III) fluoride system

The stability of curium fluoride complexes was studied using time-resolved laser fluorescence spectroscopy (TRLFS) as described in chapter 2. Fluorescence emission spectra of Cm(III) were measured of samples in the concentration range $0 < m_{NaF} < 8.8 \cdot 10^{-3}$ mol/kg H_2O with a total curium concentration in the order of 10^{-6} mol/kg H_2O. The spectrum of the Cm^{3+} aqua ion shows a maximum at 593.8 nm. When the fluoride concentration is increased, a peak appears at 601 nm corresponding to the mono-fluoride complex. This is a rather high red shift compared to that observed for other curium mono-complexes. Other complexes such as $Cm(OH)^{2+}$, $CmCl^{2+}$ and $Cm(SO_4)^+$ have emission peaks at 598.7 nm, 593.8 nm, and 596.2 nm, respectively. It is most likely due to an electronic interaction between curium and fluoride, indicating

that the bonding is not purely electrostatic. To be able to quantify the fluoride complexation, the fluorescence emissions of the spectra are deconvoluted to give the contributions from the individual species (Cm^{3+} and CmF^{2+}). The fluorescence spectra at different fluoride concentration and the spectra of the individual species Cm^{3+} and CmF^{2+} are plotted in Figure 4.2.

a)

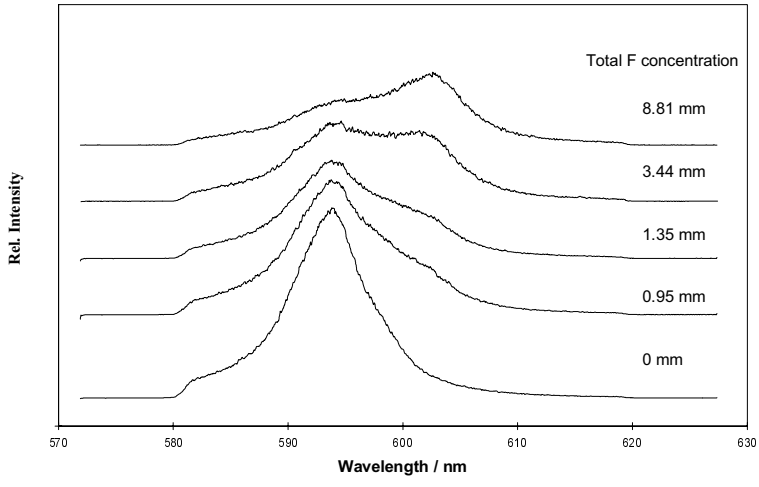

b)

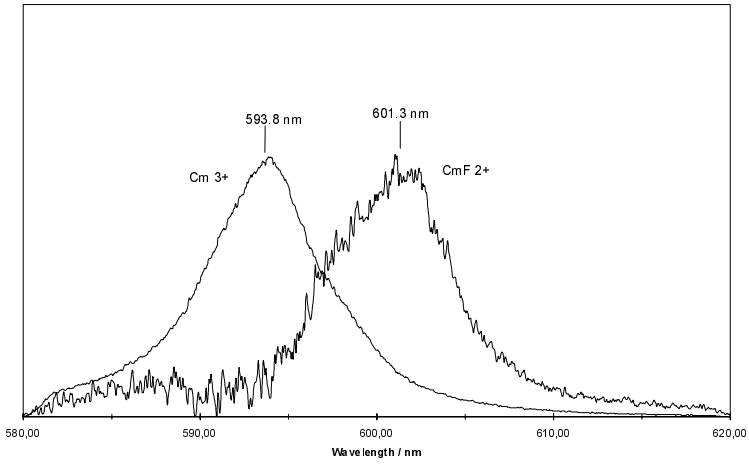

Figure 4.2. *Fluorescence emission spectra at different fluoride concentrations (top) deconvoluted into individual spectra (bottom).*

The mole fraction of CmF^{2+} is given directly by the intensity quotient of I_{CmF}/I_{tot}. The formation constant, $\log\beta_{1n}$, of the fluoride complexes can be expressed as

$$Cm^{3+} + nF^{-} \leftrightarrows CmF_n^{2+} \qquad \log\beta_{1n} = \log\frac{[CmF_n^{2+}]}{[Cm^{3+}][F^-]^n} \qquad (4.10)$$

or rewritten as

$$\log \frac{[CmF_n^{2+}]}{[Cm^{3+}]} = \log\beta_{1n} + n\log[F^-] \qquad (4.11)$$

Plotting $\log([CmF^{2+}]/[Cm^{3+}])$ against log[F] gives a straight line with slope of $n = 1$ and the complex formation constant for the monofluoro complex is $\log\beta_{1n} = 2.46 \pm 0.05$ at 1.0 molal NaCl. There is good agreement between this value and that obtained by Choppin and Unrein [54] ($\log\beta_{1n} = 2.61 \pm 0.02$ at 1.0 M $NaClO_4$), using an extraction technique. The ionic strength dependence of $\log\beta_{1n}$ has been described with a Pitzer model and the constant at zero ionic strength is calculated to be $\log \beta^0 = 3.44 \pm 0.05$. This value is comparable to the fluoride complexation of americium, $\log \beta^0 = 3.4 \pm 0.4$ [55]. At higher fluoride concentrations an additional peak appears, which is probably caused by the formation of CmF_2^+. Equilibrium data cannot be extracted for two reasons: the fraction of this peak is too small (<10%) and precipitation of CmF_3, which also contributes to the spectra. The precipitation occurs approximately at a fluoride concentration of $6 \cdot 10^{-3}$m and a curium concentration of $1 \cdot 10^{-6}$ m, indicating a solubility product ($\log K_{sp}$) in the order of 10^{-15} or lower. The same order of magnitude for $\log K_{sp}$ is observed for americium and the latest lanthanides at 0.1 ionic strength [43].

Lifetime determinations of the species were also performed. There is no significant difference in lifetime between Cm^{3+} and CmF^{2+}, in contrast to what is observed for other curium complexes. A F-H hydrogen bond may have similar quenching efficiency as the O-H bond for the coordinated water molecule

V Dynamic Studies

5.1 General background [8]

One usually says that studies of chemical kinetics have their beginning around 1850 when Ludwig Wilhelmy investigated the rate of hydrolysis of sucrose. Kinetics involves study of the rate of a chemical reaction and how the rate is influenced by concentrations of the reactants and temperature. One of the most important applications of kinetic investigations is the elucidation of reaction mechanisms. A rate equation for a chemical reaction is dependent on the concentration of one or several of the species that is present in the system of interest. The rate equation can consist of one or more terms, depending on whether the reaction proceeds through one or several parallel pathways. From the experimental rate law, the reaction mechanisms can be deduced. The mechanism will consist of a series of one or more elementary reactions. Usually, there is no unique reaction mechanism for a certain rate equation. The rate equation is used to select the most plausible choice of mechanisms by disregarding those that are not consistent with the rate law. A mechanistic choice may be corroborated by the use of additional chemical and kinetic information. In a reaction sequence there is usually one step that is much slower than the others, and it thereby controls the rate of the overall reaction, the so called rate determining step. It is impossible to obtain any kinetic information on elementary reactions following this step.

Arrhenius showed that temperature significantly effects the reactivity of a reaction. He described the relationship between the rate constant of a certain reaction and the temperature using the concept of activation energy. The reaction proceeds from reactants to products through an activated complex that has the highest potential energy along the reaction coordinates. This point is called the transition state. From the transition state, the reaction can either go to the products or back to the reactants. The transition state theory for a bimolecular reaction can be written:

$$A + B \overset{K^{\#}}{\rightleftharpoons} C^{\#} \qquad C^{\#} \xrightarrow{k^{\#}} \text{products} \qquad (5.1)$$

$K^{\#}$ is the postulated equilibrium constant between the reactant and activated complex $C^{\#}$. The rate is given by $v = k^{\#}[C^{\#}]$ or $v = k[A][B]$ where $k = k^{\#}K^{\#}$. From this theory, Eyring derived the following equation (5.2):

$$k = \frac{\kappa k T}{h} \exp\left(\frac{\Delta S^{\#}}{R}\right) \exp\left(\frac{-\Delta H^{\#}}{RT}\right) \tag{5.2}$$

where κ is the transmission coefficient (usually set to unity), k the Boltzmann and *h* the Planck constant. The activation entropy ($\Delta S^{\#}$) and enthalpy ($\Delta H^{\#}$) can easily be obtained by plotting $\ln(k/T)$ *vs.* $1/T$. The activation parameters, and the activation entropy in particular, can be used as indicators when selecting the mechanism. The transition state theory leads to the principle of microscopic reversibility which states that the forward and reverse reaction in an elementary reaction must proceed by the same mechanism.

Complex formation reactions are always ligand exchange reactions since the metal ions are solvated. The reaction is usually divided into different categories depending on whether bond breaking or bond formation takes place first and whether intermediates are identified, or not. Depending on the complex, the reaction either goes through an associative (A), dissociative (D) or an interchange mechanism (I). When the entering of the ligand is rate determining and the coordination number in transition state is increased by one, we have an associative mechanism. In a dissociative reaction, the dissociation of the ligand is rate determining and the coordination number in transition state is decreased. It may seem easy to distinguish between these two limiting mechanisms. The rate in an associative mechanism is clearly dependent on the ligand concentration, while in a dissociative pathway this is not the case. Unfortunately, a conclusion of mechanism cannot always be drawn from the observed rate law only. The solvent concentration cannot be included in the rate equation due to the large excess. A mechanism that is thought being dissociative may in fact be associative with participation of a solvent molecule. In between these two extremes, there is an interchange mechanism, often called a concerted mechanism in organic chemistry. First, an outer-sphere complex is formed and then the entering ligand moves to the inner-coordination sphere simultaneously as the leaving ligand moves to the outer sphere. Usually, the interchange mechanism has either an associative (I_a) or a dissociative (I_d) character, where either bond making or

bond breaking in the transition state is the crucial step. The activation entropy may be used to support the choice of mechanism. Generally, a large negative activation entropy indicates an associative mechanism and a positive value a dissociative mechanism [56]. However, this is not a rule, because negative entropy can for example be the result of more solvated reactants in transition state. It is therefore often more meaningful to compare the variation of activation parameters between similar reactions, than to draw conclusions from numerical values derived from only a single reaction. A further tool to deduce the correct mechanism is to determine the volume of activation $\Delta V^{\#}$ [56]. This gives much the same information as the activation entropy, but one advantage is that $\Delta V^{\#}$ is not highly influenced of how the species are solvated. The disadvantage is the experimental difficulties to obtain these data.

Catalysts lower the activation barrier; hence, the rate of the reaction is increased. The ligands in metal-complexes in aqueous solution are usually bases. The ligand exchange reactions are therefore often proton catalysed. Protonation results in a weakened M-L bond, making dissociation easier.

The rate and mechanism of a reaction are strongly dependent on the solvent. In aqueous solution, there is often a clear connection between the rates of water exchange and ligand substitution. Eigen and Wilkins [57-59] proposed a general mechanism for ligand exchange reactions where the rate determining step is the loss of water from the first coordination sphere. First, there is a fast pre-equilibrium between the complex and entering ligand (5.3) before the rate determining dissociation of water (5.4).

$$[M(H_2O)_x]^{n+} + L^{m-} \underset{}{\overset{K_{OS}}{\rightleftharpoons}} [M(H_2O)_x \cdot L]^{n-m} \qquad (5.3)$$

$$[M(H_2O)_x \cdot L]^{n-m} \xrightarrow{k_{aq}} [M(H_2O)_{x-1}L]^{n-m} + H_2O \qquad (5.4)$$

The rate of reaction is mainly dependent on the charge of the interacting species, and the interchange of ligands takes place within an outer sphere complex. In other words, the rate will not strongly depend on the nature of the entering ligand. K_{OS} is defined as the outer-sphere association constant and the overall rate can be written as in (5.5).

$$rate = \frac{k_{aq}K_{os}[M_{aq}^{n+}][L^{m-}]}{1 + K_{os}[L^{m-}]} \qquad (5.5)$$

When $K_{OS}[L^{m-}] << 1$, which is often the case, equation 5.5 can be simplified to

$$rate = k[M_{aq}^{n+}][L^{m-}], \quad k = K_{OS}k_{aq} \qquad (5.6)$$

The experimental rate constant, *k*, is a composite quantity. By estimating the association constant, K_{OS}, k_{aq} can be calculated. k_{aq} is often found to be near constant and of the same order of magnitude as the water exchange rates for the metal aqua ions. The association constant can be calculated theoretically using the Fuoss equation [60], which is based on the Debye-Hückel theory mentioned in chapter 2.

$$K_{OS} = \frac{4\pi Na^3}{3000}\exp\left(\frac{-U}{kT}\right) \qquad (5.7)$$

where,

$$U = \frac{z_1 z_2}{\varepsilon}\left[\frac{1}{a(1+\kappa a)}\right] \qquad \text{and} \qquad \kappa = \sqrt{\frac{8\pi Ne_2 I}{100\varepsilon k_B T}} \qquad (5.8)$$

N is Avogadro's number, *a* is the centre to centre distance (cm), *e* is the electron charge, k_B is the Boltzmann constant, ε is the bulk solvent dielectric constant, I is the ionic strength and z_1 and z_2 are the charge of the species. It is worth mentioning that the calculated k_{aq} by this method, and the directly measured water exchange by NMR are not really considering the same reaction. In an Eigen Wilkins mechanism, the second coordination sphere contains another ligand in addition to water. In the direct method, there are only water molecules in this sphere.

5.2 Dynamic properties of U(VI) complexes

The majority of dynamic studies done on uranyl complexes have been performed in non-aqueous solutions. The mechanism of ligand exchange reactions can differ between the media, the size, and the nucleofilic character of the ligands. Even so, some general features can be identified. The mechanisms are most commonly of interchange type, either dissociative (I_d) or associative (I_a). The exchange can also be purely dissociative, more seldom associative. A dissociative mechanism is more probable in a non-coordinating solvent than in a polar medium. In saturated complexes of type $UO_2L_5^{2+}$, where L is a unidentate ligand, the dissociation of L is the

rate determining step (L being TMP* [61], DMF [62], TMU [63], NMA [64]). Even though the rates of the reactions are independent of the ligand concentration, they are not necessarily purely dissociative. A dissociative interchange (I_d) mechanism involving the solvent is also in agreement with the experimental results. There are often simultaneously several parallel and consecutive *intra*- and *inter*-molecular reactions taking place. An i*nter*-molecular reaction is an exchange between a coordinated ligand and the bulk ligand, while an *intra*-molecular reaction is an exchange within the molecule. In the latter case, the rate of exchange is of first order with respect of the complex and independent of the concentration of entering and leaving group. The $UO_2L_5^{2+}$ complex, where L is DMSO [63], may serve as an example of parallel reactions. The rate law for the ligand exchange reaction can be written as $k_{ex} = k_1 + k_2$[DMSO]. Two different exchange paths take place, the first following a dissociative (k_1), and the second an A or I_a mechanism. There are several other examples of parallel reactions. In $UO_2(acac)_2L$ where L is DMSO, DMF, and DEF [65-68], the exchange of L follows two pathways where one is a dissociative and the other an interchange reaction. The D mechanism is dominant in acetone, while both I and D mechanisms are observed in dichloromethane [65, 67]. The *inter*-molecular acac exchange is much slower [68], and it only observed at temperature above 50°C. For comparison, the L exchange is studied in the temperature range –20°C to 30°C. The observed fast *intra*-molecular acac exchange is on the other hand [68] a result of fast external exchange of L. In the $UO_2(NIPA)_2X$ complex [69] (X is H_2O, MeOH, EtOH or Me_2CO), the exchange of X follows an interchange mechanism where the rate determining step is the exchange between an outer-sphere X and inner-sphere X. An internal exchange of the phosphoryl groups of the NIPA ligand has also been studied. The *intra*-molecular mechanism is again related to the solvent exchange. On the other hand, the *intra*-molecular NIPA exchange in the $UO_2(NIPA)_3$ complex takes place via a chelate ring opening followed by an internal assisted ligand displacement [70]. There are also a few examples of *intra*- molecular exchange reactions that take place through a rotation of the chelating ligand. This is assumed to be the case in the

*TMP = tetrametylphosphate, DMF = dimethylformamide, TMU = tetramethylurea, NMA = methylacetamid, DMSO = dimethylsulfoxide, DEF = diethylformamide, acac = acetylacetonate, NIPA = nonamethylimidodiphosphoramide, THF = Tetrahydrofutran, HMPA = hexamethylphosphoramide.

UO_2(hexafluoroacetylacetonate)$_2$X [71] complex in liquid SO_2 (X is azide, fluoroborate, THF and chloride). Kramer et al. [72, 73] have studied the same complexes in CD_2Cl_2 using X = DMSO, CH_3OH, THF, TMP, Et_3PO and HMPA. They believe that the *intra*-molecular mechanism is a migration of X and not a rotation. This mechanism does not fit with Glavincevski et al. when comparing the activation energies and the structure of the different adducts [71]. In these systems, there is also a competing *inter*-molecular reaction, which is dependent on X and the solvent.

For the uranyl aqua ion, the rate constant for the water exchange is approximately $1.4 \cdot 10^6 s^{-1}$ at 25^OC [74]. The reaction is believed to be an I_d mechanism where the uranyl-water bond breaking/bond formation takes place in the rate determining step. This type of Eigen-Wilkins mechanism is also suggested by Szabó et al. for the fluoride exchange in the binary uranyl-fluoride complexes $UO_2F_n^{2-n}$ [9]. The entering exchange partner is F^-, HF or $UO_2F_n^{2-n}$ and the breaking of a uranium-water bond is part of the rate determining step. The arguments are mainly based on the activation parameters for the different reactions. Jenkins et al. [75] also found an Eigen-Wilkins type of ligand exchange mechanism in a study done on the uranyl chlorophosphonazo system. First, it is an outer sphere complexation before a displacement of one water molecule with one of the phosphonate sites followed by the entry of the second phosphonate.

The rate and mechanism of the ligand exchange reactions seems to be strongly dependent on the number of water molecules in the inner coordination sphere. As an example, the fluoride exchange rates in $UO_2F_3(H_2O)_2^-$ [9] and $UO_2F_5^{3-}$ [76] at -5^OC are $5 \cdot 10^3$ $M^{-1}s^{-1}$ and 43 $M^{-1}s^{-1}$, respectively. Harada et al. [76] have suggested an associative or I_a mechanism for the exchange in the latter complex, this will be discussed later in section 5.3.1. The saturated binary $UO_2(CO_3)_3^{2-}$complex shows very slow kinetics. The carbonate exchange follows a dissociative mechanism with a rate constant of 1.8 s^{-1} at -5^OC [77]. The rate of exchange increases dramatically with increasing H^+ concentration. The proton catalysed pathway involves a protonation of carbonate, which increases the lability of the metal-ligand bond.

5.3 *Inter*- and *intra*- molecular exchange reactions in the $UO_2L_pF_q$ complexes.

Possible types of exchange pathways of the complexes that have been investigated in

this thesis are illustrated in Figure 5.1. In these complexes X = Y= oxygen when L denotes acetate, oxalate and carbonate; when L is picolinate, X = oxygen and Y = nitrogen. The complex is located within a solvent cage and exchange reactions may occur within the complex and/or between the coordinated and free ligands. The various types of exchange reactions have different time scales; hence, several NMR techniques were used to study them. The time-scale can be varied using different NMR active nucleus, such as ^{17}O, ^{19}F, ^{13}C or ^{1}H. The techniques are discussed in some details in chapter 2. In complexes where L is oxalate, picolinate and carbonate, the exchanges are so slow that almost every magnetically non-equivalent fluorides give rise to individual signals. This makes it possible to observe *inter*- and *intra*-molecular exchange mechanisms and isomers and isomerisation reactions as discussed below.

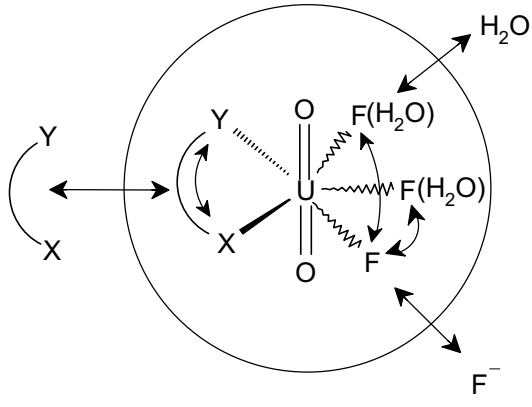

Figure 5.1*. The possible exchange pathways in the uranyl complexes.*

5.3.1 Fluoride exchange.

The fluoride exchange was mainly studied using a magnetisation transfer technique. In Figure 5.2, the exchange in the $UO_2(pic)F_3^{2-}$ complex is illustrated, where the edge fluoride F(A) is inverted. It is clearly seen from the figure that the magnetisation is transferred faster to the F(C) atom (301 s^{-1}) than to F(A), F(B) and free F. The mechanism for this *intra*-molecular reaction will be discussed later in section 5.3.2. The *inter*-molecular rate of fluoride exchange is much slower (12.8 s^{-1}). The exchange with F(B) is of the same order of magnitude and the reaction proceeds most likely via the free fluoride. Similar experiments are performed for all the complexes, and the corresponding rate constants are summarised in Table 5.1.

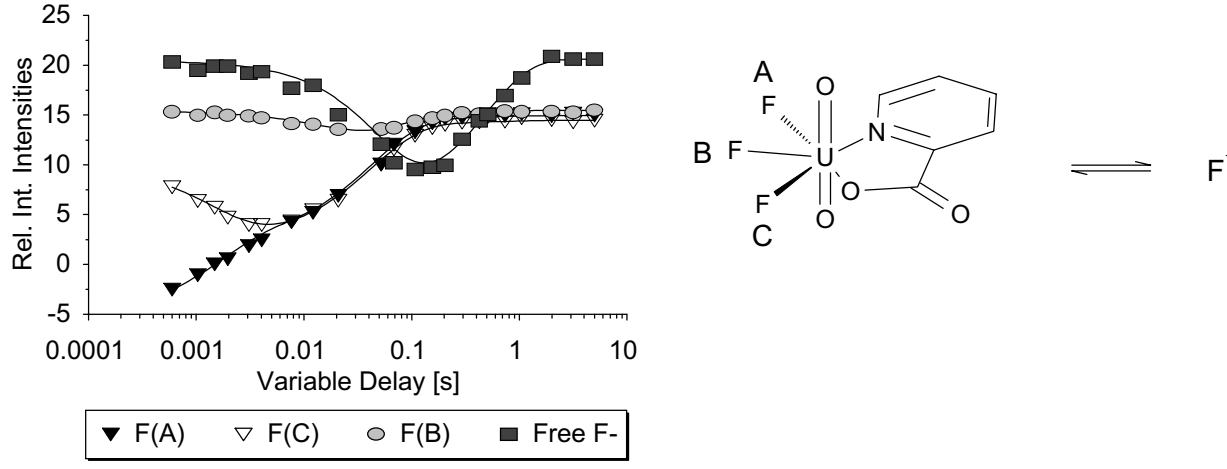

Figure 5.2*. Magnetisation transfer experiment with an inversion of the F(A) signal.*

The observed fluoride exchange rate in $UO_2(ac)F_3^{2-}$ is faster than in the other complexes, k_{obs} = 40 s^{-1}. However, this observed rate constant contains a contribution from the fluoride exchange in the binary $UO_2F_3^-$ complex due to the fast acetate exchange between these two complexes, *i.e.* the fluoride exchange takes place via two pathways, see Figure 5.3.

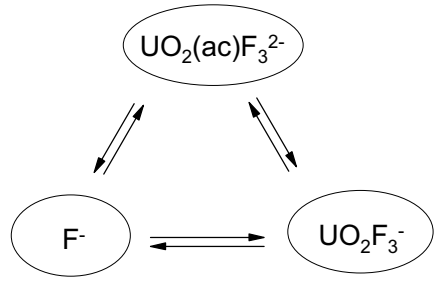

Figure 5.3. *Parallel pathways for the fluoride exchange.*

The real rate constant between $UO_2(ac)F_3^{2-}$ and F^- is of the same magnitude as the other systems, ~15 s^{-1}. All the rates are independent on the fluoride concentration indicating an exchange mechanism of either D or I_d.type. An I_a mechanism could be possible if an attack of water is rate determining. The activation parameters have been determined by Szabó and Grenthe [78]. They are approximately similar for all the oxalate and picolinate complexes with small and positive activation entropy. This

indicates that the fluoride bond breaking is more important than the water bond formation in the rate determining step, supporting an I_d mechanism.

Table 5.1.
Observed rate constants at –5 ^{0}C.

Complex	$F_{coord} \leftrightarrow F_{bulk}$	$L_{coord} \leftrightarrow L_{bulk}$	$H_2O_{coord} \leftrightarrow H_2O_{bulk}$
$UO_2(pic)F_3^{2-}$	12.8 ± 0.3[a] s^{-1}	4.7 ± 0.2 s^{-1}	
	24.4 ± 0.6[b] s^{-1}		
$UO_2(ox)F_3^{3-}$	14.1 ± 0.8[a] s^{-1}	6.2 ± 0.4 s^{-1}	
	21.6 ± 2.4[b] s^{-1}		
$UO_2(CO_3)F_3^{3-}$	15.0 ± 2.8 s^{-1}	5.7 ± 2.1 s^{-1}	
$UO_2(ox)F_2(H_2O)^{2-}$	15.8 ± 1.2 s^{-1}		1600 s^{-1}
$UO_2(ox)F(H_2O)_2^{-}$			1800 s^{-1}
$UO_2(CO_3)F_2(H_2O)^{2-}$	14.4 ± 3.0 s^{-1}		
$UO_2(pic)_2F^{-}$	12.6 ± 1.5 s^{-1}		
$UO_2(ox)_2F^{3-}$	12.3 ± 1.0 s^{-1}	8.7 ± 1.5 s^{-1}	
$UO_2(ac)F_3^{2-}$	~40-50 s^{-1}	~2050 s^{-1}	
$UO_2(ac)_3^{-}$		2750 ± 70 s^{-1}	
$UO_2(CO_3)_3^{4-}$		1.8[c] s^{-1}	
$UO_2(ox)_2(H_2O)^{2-}$		1600 ± 500 $M^{-1}s^{-1}$	
$UO_2F_5^{3-}$	43.4[d] $M^{-1}s^{-1}$		
$UO_2(H_2O)_5^{2+}$			$4.1 \cdot 10^5$ s^{-1} [e]

[a] edge fluorides, [b] central fluoride, [c] [77], [d] [76] at 25°C, [e] [74] recalculated to -5°C

In the binary uranyl-fluoride complexes [9], the fluoride exchange is much faster and follows an Eigen-Wilkins type of mechanism. The exception is the saturated $UO_2F_5^{3-}$ complex [76], where there is a slow fluoride exchange with a rate constant similar to those observed in our ternary systems. The rate is dependent on the fluoride concentration, and Harada et al. suggest an A or I_a mechanism [76]. It is difficult to study this reaction, because of the presence of fairly large concentration of $UO_2F_4^{2-}$ in the test solutions. $UO_2F_5^{3-}$ and $UO_2F_4^{2-}$ give a common signal in ^{19}F-NMR at room temperature. A high fluoride concentration is needed to coordinate five fluorides, *i.e.* about 1 M [F^-] in a 0.05 M uranyl solution to achieve approximately 1:1 ratio of $UO_2F_4^{2-}$ and $UO_2F_5^{3-}$. The main reactions involving the bulk fluoride are

$$UO_2F_4^{2-} + {}^*F^- \leftrightarrows UO_2{}^*F_4^{2-} + F^- \quad (5.9)$$

$$UO_2F_5^{3-} + {}^*F^- \leftrightarrows UO_2{}^*F_5^{3-} + F^- \quad (5.10)$$

Harada et al. [76] assume that both reactions are associative, with rate constants of $6.96 \cdot 10^3$ $M^{-1}s^{-1}$ and 43.4 $M^{-1}s^{-1}$ for reactions 5.9 and 5.10, respectively. They have expressed the observed rate constant as

$$k_{obs} = [F](k_4 + k_5 K_5[F]) / (1 + K_5[F]) \quad (5.11)$$

where k_4 and k_5 denotes the rate constants for reaction 5.9 and 510; and K_5 is the stepwise equilibrium constant. We find it more reasonable that reaction 5.10 is dissociative and have therefore tested this by rewriting the associative model in 5.11 to a dissociative type:

$$k_{obs} = [F](k_4 + k_5 K_5) / (1 + K_5[F]) \quad (5.12)$$

Comparing the two models, *c.f.* Figure 5.4, using the same numerical value for the rate constants in both models, one can clearly see that they are equivalent. Both of them are also rather insensitive to changes in k_5. The uncertainty in the numerical value should therefore be considered to be large. In order to draw conclusions on the mechanism from the data, one has to use additional data. We suggest that the close agreement between the rate constant 43.4 s^{-1} used in our model using the data of Harada et al. [76], and previously determined rate constants for the fluoride provide such evidence. It is more reasonable that the penta-fluoride complex follows a similar mechanism as in the ternary uranyl complexes. In other words, the fluoride exchange in the saturated $UO_2F_5^{3-}$ complex follows more likely a dissociative type of mechanism.

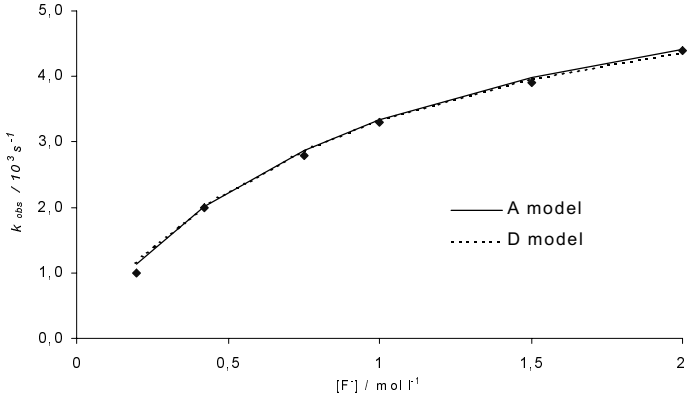

Figure 5.4 *Comparison of an D(I_d) and A(I_A) mechanism for reaction 5.10*

5.3.2 Rotation of the chelating ligand.

In the magnetisation transfer experiment of the $UO_2(pic)F_3^{2-}$ complex (Figure 5.2), we observed a faster exchange between the edge fluorides (C and A) than the external fluoride exchange. This is also seen in the ^{19}F-NMR spectrum of the complex, Figure 5.5. The middle fluoride splits into a triplet because of coupling to the two other fluorides (double doublet where two of the peaks coincide [78]), whose peaks are too

broad to show any coupling. Hence, the A-C exchange cannot occur via the free F^- ligand; the reaction is *intra*-molecular. The broadening is due to a rotation of the picolinate ligand, resulting in a site exchange of the two fluorides while F(B) is kept intact. The mechanism is illustrated as the first step in the ligand exchange reaction discussed in next section, in Figure 5.6. The first step of the picolinate rotation is a ring opening, believed to take place at the uranium-nitrogen bond.

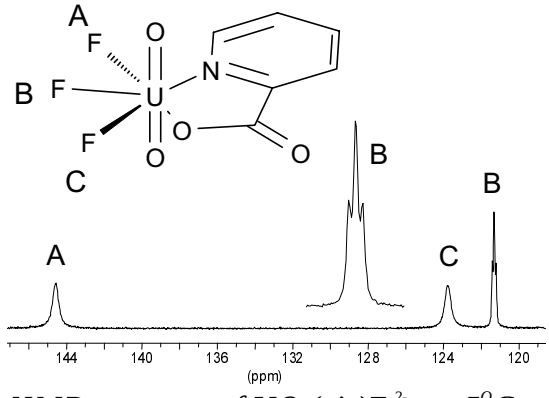

Figure 5.5. *^{19}F NMR spectrum of $UO_2(pic)F_3^{2-}$ at –5^{O}C.*

The hypothesis was tested using different picolinate derivatives. The rate of exchange increases when an electron-withdrawing group (NO_2) and the rate decreases in the presence of an electron donating group (3-pentyl) in the para position of the pyridine ring. It is believed that these substituents on the aromatic ring mainly influence the electron density around the nitrogen atom and therefore the strength of the U-N bond. The rate determining step is therefore believed to be an U-N bond breaking followed by a fast ligand rotation and ring closure. In an additional study done by Szabó and Grenthe [78], the activation parameters were determined. They found a large variation in $\Delta S^{\#}$ between the different substituted picolinate ligands. This indicates a varying degree of water participation in transition state. The picolinate ring opening is believed to be water assisted; this is compatible with a water exchange that is faster than the rate rotation. A ligand rotation is also observed in the $UO_2(pic)_2F^-$ complex and explains the exchange between the different isomers. They are illustrated in chapter 3, Figure 3.6. The isomers were only detected when the complex was dissolved in methanol; it was then possible to decrease the temperature to -54°C. The rotation rate is calculated to be approximately 1500 s^{-1} at -5^{o}C, which is 5 times faster than in the $UO_2(pic)F_3^{2-}$ complex. The activation entropy is

highly negative, $\Delta S^{\#}$ = -82.9 J mol^{-1} K^{-1} (erroneously given a positive value in the paper). The difference in the picolinate rotation rate between $UO_2(pic)_2F^-$ and $UO_2(pic)F_3^{2-}$ could be due, either to more crowded coordination sphere or simply to the use of two different solvents. The latter explanation seems more likely. The activation entropy for the rotation in $UO_2(pic)_2F^-$ is larger in dimethyl sulfoxide ($\Delta S^{\#}$ = -27.8 J mol^{-1} K^{-1}) [78] as compared to both methanol and water solutions.

5.3.3. Exchange of the bidentate, chelating (X-Y) ligand

For the oxalate and carbonate complexes, it was possible to perform ^{13}C-NMR inversion transfer experiments using ^{13}C enriched oxalate and carbonate. The picolinate exchange was studied using ^{1}H-NMR. For the UO_2-acetate-fluoride system, it was not possible to observe separate peaks for free and coordinated acetates due to the large excess of acetate. An indirect way of observing this ligand exchange could be achieved using ^{19}F-NMR. The fluoride peaks in the $UO_2(ac)F_3^{2-}$ complex are much broader than that due to the fluoride exchange alone; the additional broadening is caused by acetate exchange, as described in Figure 5.3. The mechanism of ligand exchange is assumed to be sequential, with first a ring opening with a possibility for water to coordinate before breaking the second bond seen in Figure 5.6.

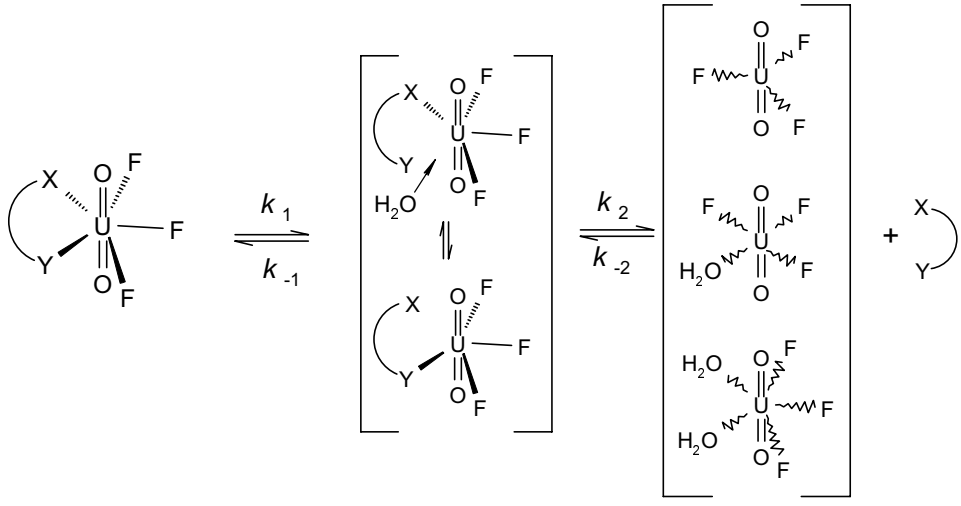

Figure 5.6*. Mechanism for ligand exchange in UO_2LF_3.*

The mechanisms are unlike in the different ternary systems investigated. Acetate dissociates completely from the complex, allowing water to approach the inner coordination sphere, hence the intermediate $UO_2F_3(H_2O)_2^{2-}$ is formed. Support

for this is obtained by observing how the line broadening of this peak depends on the acetate concentration. For the other ligands, different intermediate/transition states are formed with a smaller number of coordinated water as in $UO_2F_3(H_2O)^-$ or $UO_2F_3^-$ [78]. The rate determining step for picolinate exchange in the $UO_2(pic)F_3^{2-}$ complex is the second step, k_2 in Figure 5.6. Ring opening is a fast reaction (300 s^{-1}), while the *inter*-molecular exchange rate is much slower, 4.2 s^{-1}. Oxalate is bonded stronger than picolinate, and it is assumed that the rate determining step for oxalate exchange in $UO_2(ox)_2F^{3-}$ is the ring opening [78]. The conclusion is based on the known oxalate exchange in the binary $UO_2(ox)_2(H_2O)$ described below. If the rate determining step in the ternary system is k_2, the mechanism would be similar to the binary one, which is not the case.

Binary systems. To obtain further insight into the mechanism of the ligand exchange reactions, binary oxalate and acetate systems were studied as well. Since acetate is a small ligand, uranyl can coordinate three acetates giving the stable saturated trisacetate, $UO_2(ac)_3^-$, complex. Oxalate on the other hand, forms $UO_2(ox)_2(H_2O)^{2-}$ as the main complex at high oxalate concentrations. The ligand exchange reactions for the two different $UO_2L_2(H_2O)$ (L = ac and ox) complexes seem to follow similar Eigen-Wilkins type of mechanism, *c.f.* Figure 5.7.

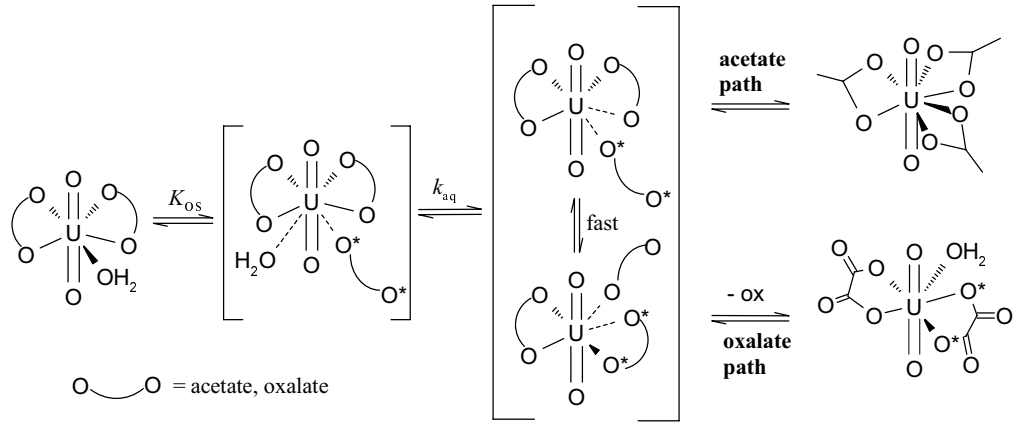

Figure 5.7*. Mechanism of oxalate/acetate exchange in $UO_2L_2(H_2O)$.*

The water exchange rate can be calculated using equation 5.5, to give k_{aq} is $1.3 \cdot 10^6$ s^{-1} and $2.9 \cdot 10^6$ s^{-1} for L = acetate and oxalate, respectively. These values are comparable with the water exchange rates for the aqua ion, $k = 4.1 \cdot 10^5$ s^{-1} [74], which supports the mechanistic choice. From the concept of microscopic reversibility follows that the

dissociation of acetate in the $UO_2(ac)_3^-$ complex must be water assisted. The fact that a rate equation is independent on the ligand concentration does not simply imply that the mechanism is dissociative.

5.3.4 Proton catalysed reactions**.**

The ligand exchange reactions for the saturated complexes $UO_2(CO_3)_3^{2-}$ [77], $UO_2(CO_3)F_3^{3-}$, $UO_2(ox)F_3^{3-}$, $UO_2(ox)_2F^{2-}$ [78] and $UO_2(ac)_3^-$ are all proton catalysed. The effect is largest when the most basic ligand carbonate is used and smallest for oxalate, Figure 5.8. While there is a clear connection between the catalytic effect and the basicity when carbonate and oxalate are the reacting ligands, the proton catalysis of the acetate exchange is stronger than the base constant for acetate indicates.

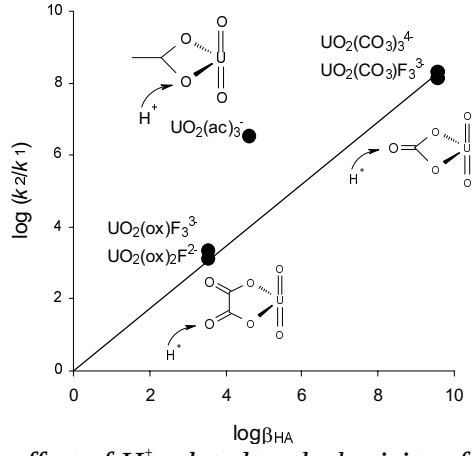

Figure 5.8*. The catalytic effect of H^+ related to the basicity of the ligands.*

The reason is believed to be that acetate has both of its oxygen atoms coordinated to uranyl. The other ligands have non-coordinating oxygen atoms, which are exposed to proton attack. Protonation of coordinated oxygen is expected to be more effective. The H^+/D^+ isotope effect has been studied for the $UO_2(ox)_2F^{3-}$ [78] and $UO_2(CO_3)^{4-}$ [77] complexes. The ligand exchange rates in both complexes are more effectively catalysed by D^+. This is a clear indication of a pre-equilibrium between the complex and a proton before the dissociation of the ligand.

5.3.5 Isomerisation reactions in $UO_2LF_2(H_2O)$ and $UO_2LF(H_2O)_2$

In $UO_2LF_2(H_2O)$, there are three possible isomers when L is picolinate. When X = Y as in the oxalate and carbonate complexes, two of the isomers are identical (Figure 5.9).

In the case when L is oxalate, the three magnetically different fluorides are distinguished at -5^{0}C.

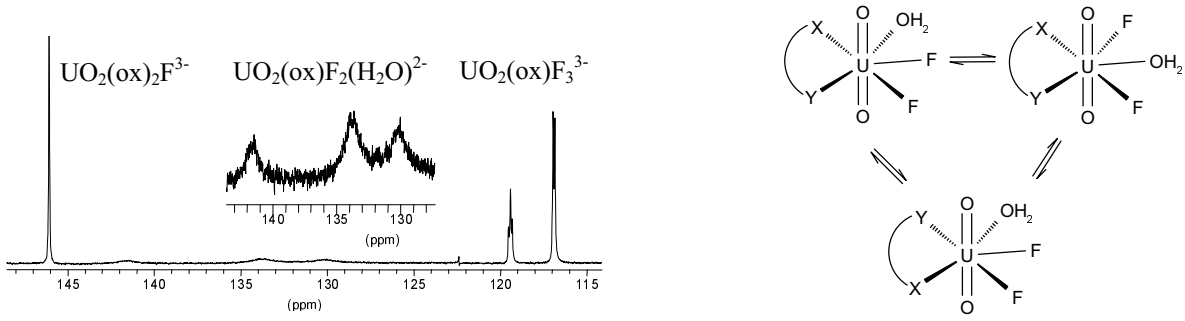

***Figure 5.9**. [19]F-NMR spectrum of a solution containing 5 mM UO_2^{2+}, 10 mM oxalate, 20 mM fluoride at pH = 6.5 and at -5 ℃ and the different isomers of $UO_2LF_2(H_2O)$.*

It is clearly seen from the [19]F-NMR spectrum that the peaks, originating from the water-containing complexes, are much broader than those from the other complexes. The broadening cannot be explained by an *inter*-molecular fluoride or oxalate exchange, because these rates are too slow, see Table 5.1. A site exchange between coordinated water and fluoride is the most likely explanation for the observed line broadening. This exchange probably takes place via an *inter*-molecular water exchange. The rate constant, estimated from the line broadening is approximately 1600 s^{-1}, which is 2 orders of magnitude slower than the water exchange for the hydrated uranyl ion at the same temperature [74]. When picolinate and carbonate were used as ligands, it was not possible to observe all the isomers because of overlapping fluoride peaks. For the acetate system, isomers cannot be identified because of too fast acetate exchange.

For the $UO_2LF(H_2O)_2$ system, it was only possible to obtain information of isomers for L = oxalate. There are two possible isomers, identified in the fluoride spectrum shown in Figure 5.10.

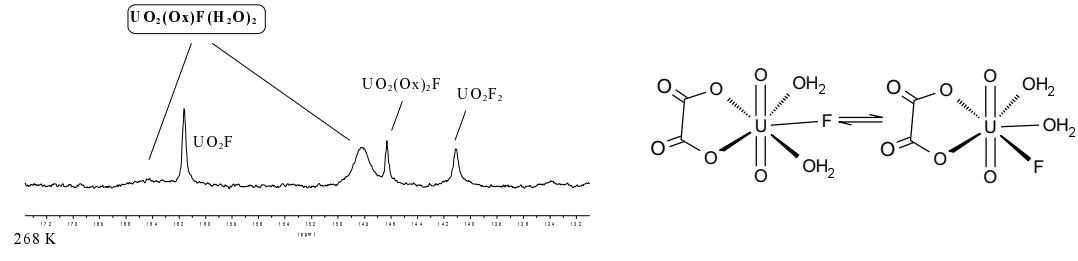

***Figure 5.10.** The isomers of $UO_2(ox)F(H_2O)_2^-$ and the [19]F-NMR spectrum of a solution containing 5 mM UO_2^{2+}, 5 mM oxalate, 3 mM fluoride at pH = 4.4 and at –5^{0}C.*

The narrow lines observed for the other complexes indicate that the exchange between the isomers do not involve binary complexes, but occurs via slow water exchange, as for the $UO_2(ox)F_2(H_2O)^{2-}$ complex. The rate constant for the water exchange is estimated, 1800 s^{-1}, which is close to the value obtained for $UO_2(ox)F_2(H_2O)^{2-}$.

The water exchange rate is strongly dependent on the other ligand coordinated to uranyl, which slow down the water dissociation. There are very few studies done in this field. Ikeda et al. [79] observed similar trend in the uranyl-DMSO-water system where the water exchange rate decreased one order of magnitude as a result of DMSO coordination. One may speculate on the possible reasons for the slow rate of exchange in the complexes described above as compared to that in $UO_2(H_2O)_5^{2+}$. We have explored the possibility of *intra*-molecular hydrogen bonding between the coordinated water and coordinated fluoride or carboxylate oxygen. From the known structure of uranium (VI) complexes, we can estimate the distances between the coordinated oxygen in a water molecule and the neighbouring carboxylate oxygen or fluoride to ~2.8Å. This is a typical distance between a hydrogen bond donor (such as water) and acceptor in solid state structures. In a previous study, Wahlgren et al [80] has made quantum chemical calculations at the *ab initio* level on the structure of the $UO_2(H_2O)_5^{2+}$ ion and the energy differences between different orientations of the coordinated water molecules. It turned out that the highest energy is obtained when the water molecules, including their hydrogen atoms, are all in the equatorial plane, point group D_{5h}. A substantially lower energy is obtained if at least one of the coordinated water molecules is rotated around an axis in the coordination plane so that one hydrogen atom is above and the other below this plane. To test the possibility of formation of an *intra*-molecular hydrogen bonding, Wahlgren et al. [81] have recently made a geometry optimisation of $UO_2(H_2O)_5^{2+}$ in C_{5h} geometry. It turned out that the optimal geometry for hydrogen bond formation, *c.f.* Figure 5.11, had the highest total energy. There was a substantial decrease in energy, more than 100 kJ/mol, when the water molecules were rotated by an angle α around an axis through the water oxygens and perpendicular to the coordination plane, *c.f.* Figure 5.11.

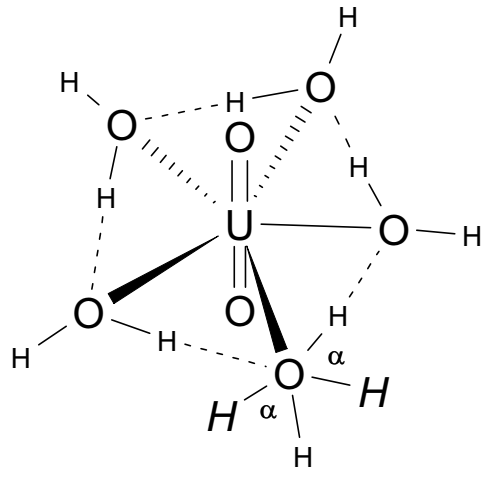

***Figure 5.11**. Geometry optimisation of $UO_2(H_2O)_5^{2+}$ in C_{5h} geometry.*

These findings indicate very clearly that the strong electrostatic repulsion between UO_2^{2+} and the water hydrogen prevents the formation of hydrogen bond. However, the situation might be different in the fluoride complexes, both because fluoride is a stronger hydrogen bond acceptor than oxygen and because of the total negative charge of the complex. There are on going *ab initio* studies on these complexes trying to judge whether hydrogen bonds may be form in the presence of coordinated fluoride.

5.4 Dynamic properties of ternary Th(IV) EDTA complexes

Fluoride NMR was an important tool in the dynamic studies done on the ternary complexes described above. It has been used not only for direct observation of the fluoride exchange reactions, but also indirectly to study other reactions, such as isomerisation and water exchange reactions. It was therefore of interest to investigate whether this method could be applied on other actinide systems. Thorium is a natural choice as a representative for the tetravalent actinides. Thorium has only one oxidation state and it is less easy hydrolysed than for example U(IV). In the ternary UO_2-L-F (L = ox, pic, ac and CO_3^{2-}) systems, the detailed kinetics was observed because either no water was presented in the inner coordination sphere or because the rate of water exchange was slowed down. To create thorium complexes with few coordinated water molecules, it was necessary to use a polydentate ligand. It is well known that EDTA forms strong complexes with thorium. Ternary complexes are

known, Th(EDTA) binds readily up to two fluorides [82, 83] and hydroxides [84, 85]. EDTA complexes have a variety of possible structures [86]. It may act as a bridging ligand and the stereochemistry of the chelate may differ.

The ^{1}H-NMR spectra of the ternary Th-EDTA-fluoride system show a typical AB quartet of the EDTA ligand. At high fluoride concentration there is a decrease in the amount of complexed EDTA and an increase in bulk EDTA indicating a substitution of the EDTA ligand with fluoride. This is also observed in the ^{19}F-NMR spectra where the intensities decrease due to the formation of ThF_4 precipitate. The ^{19}F-NMR studies confirm complexation of two fluorides to the Th(EDTA) complex as previously observed using potentiometry [82]. The complexes $Th(EDTA)F^-$ and $Th(EDTA)F_2^{2-}$ are in fast exchange with one another on ^{1}H-NMR time scale. On the other hand, they give rise to separate peaks in ^{19}F-NMR. These peaks are broader than expected from the fluoride exchange . The broadening cannot be caused by an exchange between the complexes, as seen in the binary uranyl-fluoride system [9], because the peaks are also broad in solution containing only one predominant thorium complex. It is probably caused by an *intra*-molecular rearrangement of the EDTA ligand. To obtain information of the rate of *inter*-molecular fluoride exchange, one can only use the line with of the free fluoride peak. The most likely exchange reactions are written in equation 5.13-5.15.

$$Th(EDTA)F^- + {}^*F^- \underset{}{\overset{k_1}{\rightleftharpoons}} Th(EDTA){}^*F^- + F^- \qquad (5.13)$$

$$Th(EDTA)F^- + F^- \underset{k_3}{\overset{k_2}{\rightleftharpoons}} Th(EDTA)F_2^{2-} \qquad (5.14)$$

$$Th(EDTA)F_2^{2-} + {}^*F \underset{}{\overset{k_4}{\rightleftharpoons}} Th(EDTA){}^*F_2^{2-} + F^- \qquad (5.15)$$

The change in line with of the bulk fluoride with changing concentration of the reactants was used to obtain the rate constant; $k_4 = (7.1 \pm 0.8)10^3\ M^{-1}\ s^{-1}$ and $(2k_1+k_2) = (6.8 \pm 0.5)10^4\ M^{-1}s^{-1}$. It is not possible to distinguish between $k_1$and k_2 using the free fluoride signal. k_4 is much slower than the rate of fluoride attack on Th(EDTA)F. The saturated $Th(EDTA)F_2$ is less likely to participate in a reaction with fluoride, similar to what is observed in the uranyl system. It is difficult to know whether this reaction actually is a fluoride exchange or not, it can just as well be the first step in the substitution of EDTA.

VI Conclusions

There are two main findings described in this thesis; first of all the identification of stable ternary uranyl complexes and secondly, that it has been possible to obtain mechanistic information on a variety of detailed exchange reactions not observed in aqueous solution before.

The ligand exchange mechanisms in aqueous solutions are strongly dependent on whether water is present in the inner coordination sphere, or not. When it is eliminated, much slower kinetics and *intra*-molecular reactions can be observed. Most of the observed reactions take place via a dissociative or dissociative interchange mechanism. There are no examples of pure associative mechanisms. ^{19}F-NMR turned out to be a powerful technique to study these reactions due to the sensitivity, the large chemical shift differences and of the possibility to use ^{19}F as a spy nucleus to observe reactions where fluoride is not directly involved in the mechanism. In complexes where water is coordinated, water usually plays a crucial part in the mechanism. The rate of water exchange is important for the overall rate of exchange of other ligands. A very interesting observation is that the water exchange rate is two order of magnitude slower in the complexes of type $UO_2(ox)F_n(H_2O)_{2-n}$ as compared to the water exchange rate in the uranyl aqua ion.

Most of the thermodynamic studies on actinide complexes are done on the binary systems; hence, the databases contain mainly information of this type. In this context, it is important to notice that the ternary fluoride complexes studied in this thesis turned out to be very stable. The stepwise fluoride constants are surprisingly high and comparable, after corrected for the statistical factor, with those in the binary system. This indicates that electrostatic forces are not the only driving forces in the complex formation reactions. The data presented here can make it possible to develop reasonable theories of the composition, stoichiometry and stability constants of the ternary complexes that might be formed in multicomponents systems as encountered *e.g.* in natural aquatic systems. The estimated formation constant can be obtained by simply adding the constants of the corresponding binary complexes and correcting for the statistical factor. A factor ten in the formation constant can be critical on whether a specie is formed in significant amounts, or not. The proposed

methods are not accurate enough to predict constants that well. If a complex seems to appear in large concentrations, lab studies are needed to verify if these complexes are formed or not.

The complex formation reactions are fast compared to the rate of the transportation in ground and surface water systems. This means that the rate of migration is mainly dominated be hydrological processes. The situation is totally different when separation technology is used, such as in the solvent extraction processes. The rate in this case can be controlled by chemical reactions and not by diffusion. Liquid-liquid extraction is the standard technique for reprocessing used nuclear fuel. Chemical dynamics plays a much more important role in redox reactions. In particular in one or two electron transfer reactions where there is simultaneously a change in structure or constitution. These reactions are usually very slow. Examples are the redox reactions between U(IV) and U(V) or between U(IV) and U(VI). On the other hand, the redox reactions between U(III) and U(IV) or U(V) and U(VI) are fast. These processes are studied by other members in our group [74].

Outlook on future work

The coordination chemistry of the actinides is by no means fully understood. It is probably more correct to say that the understanding of the 5*f*-elements only have started to emerge. Several interesting questions are arisen in this thesis, such as:

- What is really controlling the rate of water exchange? Crystal structures of complexes of type $UO_2LF_n(H_2O)_{2-n}$ could possibly establish some further insight. *Ab initio* calculations may also be very helpful. Continued work on the kinetics, obtaining activation parameters *etc.* might also be useful. Some work along these lines is going on in our group.
- The fluoride bonding does not seems to be driven only by electrostatic interactions, neither in UO_2^{2-} or Cm^{3-} complexes, where one would expect strong hard / soft interactions. Not much is known of the type of bonding in the actinide complexes. Continued experimental as well as quantum chemical calculation on various types of complexes will result in a deeper understanding of this issue.
- We believe that the fluoride exchange in the saturated binary $UO_2F_5^{3-}$ complex follows a dissociative type of mechanism in contrast to an associative suggested

by Harada et al. [76]. The rate constant is also poorly estimated. Further studies are here necessary.

- The mechanism of exchange of the bidentate, chelating ligand is not clear. In the picolinate case it is true that the breaking of the second bond in the chelate that is rate determining. For the ligands where the bidentate contains to donors that are of same strength the picture is not that clear. It seems that both the weaker bonded acetate and the stronger bonded oxalate exchange with a rate determining ring opening. Further studies may be needed to draw any more definite conclusions.
- The thorium(IV)-EDTA work indicated that there is fluxionality in the coordinated EDTA ligand. To be able to obtain detailed information of these processes, it is probably necessary to make substitutions in the ligand, making it less symmetrical. There are also other potential polydentate ligands that could be used. It is of great interest to obtain more kinetic and thermodynamic information of the tetravalent actinides.

In the curium(III) system, there should be possibilities to form ternary complexes to be formed. When predicting whether these exist, using carbonate as the example of the second ligand, it seems likely that $Cm(CO_3)_pF_q$ complexes are formed in a broad concentration range. It will be difficult to obtain kinetic information for the *f*-elements in oxidation state III, but it should be possible to use lanthanides as models, because they have many similar properties as the actinides in the same oxidation state.

Acknowledgement

First of all, I want to show my sincere gratitude to my supervisor Ingmar Grenthe. I have been very satisfied with your guiding throughout these four years, not only due to your enormous knowledge in chemistry and your working capacity, but just as much because of your always open door and good sense of humour. I have also appreciated your humble and open minded attitude towards science. These are, in my opinion, two crucial qualities for being a good scientist, which you indeed are. **Tack så mycket!**

My co-author and roommate Zoltán Szabó is greatly acknowledged for teaching me all I know in dynamic NMR spectroscopy and for all our scientific and less scientific discussions. It has been a pleasure to work with you. **Köszönöm!**

Part of the work was done in Germany, and I am grateful to Thomas Fanghänel at the research centre Karlsruhe (FZK) for welcoming me and teaching me the fluorescence spectroscopy. **Vielen Dank!** The single crystal X-ray diffraction was done at the University of Lund and Maria Johansson and Åke Oskarsson are thanked for their cooperation. **Tack!**

I would like to thank my sponsors: Swedish Natural Science Research Council (NFR) for my scholarship the first one and a half years and KTH for paying my salary the last years, Ragnar and Astrid Signeuls foundation and Frans Georg and Gull Liljenroths foundation for financing my trips to Germany and Japan, respectively.

The first doctor in “kollegiet”, Morten Sørlie, has thoroughly read through this thesis and given me good comments and corrections. **Tusen takk!** Thanks also to Henry Moll for reading this thesis and for making it a pleasure to come to work. **Vielen Dank!** Maria José Gonzalez is also acknowledged for doing some proof reading, for teaching me how to work more analytical, for always updating me with tricks in the computer world, and simply for being my best friend in Stockholm. **Muchas gracias!**

Finally, but not the least, I want to thank my previous and present colleges and friends at inorganic chemistry, especially the lunch and pizza companions for all our “fruitful discussions”. **Thank you!**

References

(1) Martell, A. E. *Coordination ChemistryACS Monograph 168*; Van Nostrand Reinhold Company: New York, 1971.

(2) Martell, A. E. *Coordination ChemistryACS Monograph 174*; American Chemical Society: Washington, 1978.

(3) Rossotti, F. J. C.; Rossotti, H. *The Determination of Stability Constants and Other Equilibrium Constants in Solution*; McGraw-Hill Book Company, Inc.: New York, 1961.

(4) Grenthe, I.; Fuger, J.; Konings, R. J. M.; Lemire, R. M.; Muller, A. B.; Ngyen-Trung, C.; Wanner, H. *Chemical Thermodynamics of Uranium*; North-Holland: Amsterdam, 1992.

(5) Fuger, J.; Khodakovsky, I. L.; Sergeyeva, E. I.; Medvedev, V. A.; Navratil, J. D. *The chemical Thermodynamics of Actinide Elements and Compounds*; IAEA: Vienna, 1992.

(6) Bjerrum, N. *Kgl. Danske Videnskab. Selskabs. Skrifter Naturvidenskab. mat. Afdel 7* (1915) 4.

(7) Bjerrum, N. *Z. Anorg. u. Allgem. Chem. 119* (1921) 54.

(8) Katakis, D.; Gordon, G. *Mechanisms of Inorganic Reactions*; John Wiley & Sons: New York, 1987.

(9) Szabó, Z.; Glaser, J.; Grenthe, I. *Inorg. Chem. 35* (1996) 2036.

(10) Sillén, L. G.; Warnquist, B. *Ark. Kemi 31* (1969) 315.

(11) Sillén, L. G. In *Coordination Chemistry ACS Monograph 168*; Martell, A. E., Ed.; Van Nostrand Reinhold Company: New York, 1971; Vol. 1.

(12) Helgeson, H. C.; Kirham, D. H.; Flowers, G. C. *Am. J. Sci. 281* (1981) 1249-1516.

(13) Grenthe, I.; Spahu, K.; Plyasonov, A. V. In *Modelling in Aquatic Chemistry*; Grenthe, I., Puigdomenech, I., Eds.; OECD Nuclear Energy Agency (NEA): Paris, 1997, pp pp. 325-426.

(14) Ciavatta, L. *Ann. Chim. 70* (1980) 551-567.

(15) Pitzer, K. S. *Ion Interaction Approach: Theory and Data Correlation.*, 2 ed.; CRC Press, 1991.

(16) Kimura, T.; Choppin, G. R. *J. Alloys Comp. 213/214* (1994) 313.

(17) Kim, J. I.; Klenze, R.; Wimmer, H.; Runde, W.; Hauser, W. *J. Alloys and Compounds 213/214* (1994) 333.

(18) Paviet, P.; Fanghänel, T.; Klenze, R.; Kim, J. I. *Radiochim. Acta 74* (1996) 99.

(19) Fanghänel, T.; Kim, J. I. *J. Alloys and Compounds 271-273* (1998) 728.

(20) Sandström, J. *Dynamic NMR Spectroscopy*; Academic Press: London, 1982.

(21) Orrell, K. G.; Šik, V.; Stephenson, D. *Progress in NMR Spectroscopy 22* (1990) 141.

(22) Stout, G. H.; Jensen, L. H. *X-ray Structure Determination*, second ed.; John Wiley & Sons: New York, 1989.

(23) Kauffman, G. B. In *Nobel Prize Topics in Chemistry*; van Spronsen, J. W., Ed.; Heyden & Son Ltd: Cambridge, 1981.

(24) Cotton, F. A.; Wilkinson, G. *Advanced Inorganic Chemistry*, fifth ed.; John Wiley & sons: New York, 1988.

(25) Bois, C.; Dao, N. Q.; Rodier, N. *Acta Crystallogr. B32* (1976) 1541.

(26) Honan, J. G.; Lincoln, S. F.; Williams, E. H. *Inorg. Chem. 17* (1978) 1855.

(27) Åberg, M.; Ferri, D.; Glaser, J.; Grenthe, I. *Inorg. Chem. 22* (1983) 3986.

(28) Zachariasen, W. H. *Acta. Crystallogr. Sect. C 7* (1954) 783.

(29) Bombieri, G.; De Paoli, G. In *Handbook on the Physics and Chemistry of the Actinides*; Freeman, A. J., Keller, C., Eds.; Elsevier Science Publishers B.V.: Amsterdam, 1985; Vol. 3.

(30) Clark, D. L.; Hobart, D. E.; Neu, M. P. *Chem. Rev. 95* (1995) 25
and references within.

(31) Zachariasen, W. H.; Plettinger, H. A. *Acta. Crystallogr. Sect. C 12* (1959) 526.

(32) Alcock, N. W. *J. Chem. Soc. Dalton* (1973) 1614.

(33) Alcock, N. W. *J. Chem. Soc. Dalton* (1973) 1610.

(34) Denning, R. G. In *Handbook of Inorganic Chemistry, General Properties Uran*; Gmelin, 1983; Vol. A6, pp 37-71.

(35) Roof, R. B.; Cromer, D. T.; Larson, A. C. *Acta. Cryst. 17* (1964) 701.

(36) Cousson, A.; Nectoux, F.; Pagés, M.; Rizkalla, E. N. *Radiochimica Acta 61* (1993) 177.

(37) Alcock, N. W.; Kemp, T. J.; Roe, S. M.; Leciejewicz, J. *Inorg. Chim. Acta 248* (1996) 241.

(38) Silverwood, P. R.; Collison, D.; Livenes, F. R.; Beddoes, R. L.; Taylor, R. J. *J. Alloys Comp. 271-273* (1998) 180.

(39) Dao, N. Q.; Bkouche-Waksman, I.; Walewski, M.; Caceres, D. *Bull. Soc. Chim. Fr. No 3-4* (1984) I-129.

(40) Ahrland, S.; Chatt, J.; Davies, N. R. *Quart. Rev. 12* (1958) 265.

(41) Bjerrum, J. *Metal Amine Formation in Aqueous solution. Theory of the Reversible Step Reactions*; P. Haase and son: Cobenhagen, 1957.

(42) Grenthe, I.; Hummel, W.; Puigdomenech, I. In *Modelling in Aquatic Chemistry*; Grenthe, I., Puigdomenech, I., Eds.; OECD Nuclear Energy Agency (NEA): Paris, 1997, pp pp. 69-130.

(43) Martell, A. E.; Smith, R. M.; Motekaitis, R. J. *Critical Selected Stability Constants of Metal Complexes Database;* Texas A&M University, 1997.

(44) Brown, D. In *Chapter 45 of Comprehensive Inorganic Chemistry*
The Chemistry of the Actinides; Bailar, J. C., Emeleus, H. J., Nyholm, R., Trotman-Dickenson, A. F., Eds.; Pergamon Press: Oxford, 1973; Vol. 10.

(45) Ahrland, S. In *The Chemistry of the Actinede Elements*; Katz, J. J., Seaborg, G. T., Morss, L. R., Eds.; Chapman and Hall Ltd: Bristol, 1986; Vol. 2.

(46) Ahrland, S. *Acta Chem. Scand. 5* (1951) 199.

(47) Havel, J. *Chem. Commun. 34* (1969) 3248.

(48) Grenthe, I.; Ferri, D.; Salvatore, F.; Riccio, G. *J. Chem. Dalton Trans.* (1984) 2439.

(49) Grenthe, I.; Lagerman, B. *Radiochimica Acta 61* (1993) 169.

(50) Katkar, V. S.; Munshi, K. N. *Indian J. Chem. 24A* (1985) 677.
and references within.

(51) Ahrland, S.; Kullberg, L. *Acta Chem. Scand. 25* (1971) 3457.

(52) Ahrland, S.; Kullberg, L. *Acta Chem. Scand. 25* (1971) 3677.

(53) Templeton, D. H.; Zalkin, A.; Ruben, H.; Templeton, L. K. *Acta Cryst. C 41* (1985) 1439.

(54) Choppin, G. R.; Unrein, P. J. In *Transplutonium Elements*; Muller, W., Lindner, R., Eds.; North Holland Publishing Company: Amsterdam, 1976, pp 97-107.

(55) Silva, R. J.; Bidoglio, G.; Rand, M. H.; Robouch, P. B.; Wanner, H.; Puigdomenech, I. *Chemical Thermodynamics of Americium*; North Holland: Amsterdam, 1995.

(56) Lincoln, S. F.; Merbach, A. E. In *Advances in Inorganic Chemistry;* Sykes, A. G. Eds.; Academic Press: London, 1995.

(57) Eigen, M. *Electrochem. 64* (1960) 115.

(58) Wilkins, R. G.; Eigen, M. *Adv. Chem. Ser. 49* (1965) 55.

(59) Richens, D. T. *The Chemistry of Aqua Ions*; John Wiley & Sons Ltd.: Chichester, 1997.

(60) Fouss, R. M. *J. Am. Chem. Soc. 80* (1958) 5050.

(61) Crea, J.; Digiusto, R.; Lincoln, S. F.; Williams, E. H. *Inorg. Chem. 16* (1977) 2825.

(62) Bowen, R. B.; Lincoln, S. F.; Williams, E. H. *Inorg. Chem. 15* (1976) 2126.

(63) Ikeda, I.; Tomiyasu, H.; Fukotomi, H. *Bull. Res. Lab. Nucl. Reactors 4* (1979) 47.

(64) Honan, G. J.; Lincoln, S. F.; Williams, E. H. *Inorg. Chem. 17* (1978) 1855.

(65) Ikeda, Y.; Tomiyasu, H.; Fukutomi, H. *Bull. Chem. Soc. Jpn. 56* (1983) 1060.

(66) Ikeda, Y.; Tomiyasu, H.; Fukutomi, H. *Inorg. Chem. 23* (1984) 1356.

(67) Ikeda, Y.; Tomiyasu, H.; Fukutomi, H. *Bull. Chem. Soc. Jpn. 57* (1984) 2925.

(68) Ikeda, Y.; Tomiyasu, H.; Fukutomi, H. *Inorg. Chem. 23* (1984) 3197.

(69) Rodehüser, L.; Rubini, P. R.; Bokolo, K.; Delpuech, J.-J. *Inorg. Chem. 21* (1982) 1061.

(70) Bokolo, K.; Delpuech, J.-J.; Rodehüser, L.; Rubini, P. R. *Inorg. Chem. 20* (1981) 992.

(71) Glavincevski, B.; Brownstein, S. *Inorg. Chem. 22* (1983) 221.

(72) Kramer, G. M.; Dines, M. B.; Kastrup, R.; Melchior, M. T.; Maas Jr, E. T. *Inorg. Chem 20* (1981) 3.

(73) Kramer, G. M.; Maas Jr, E. T. *Inorg. Chem 20* (1981) 3514.

(74) Bányai, I.; Farkas, I.; Grenthe, I.; Szabó, Z. "The Rates and Mechanisms of Water exchange of UO_2^{2+}: A variable Temperature ^{17}O-NMR study" *In preparation* (1999).

(75) Jenkins, J. F.; Sullivan, J. C.; Nash, K. L. *Radiochim. Acta 68* (1995) 209.

(76) Harada, M.; Fujii, Y.; Sakamaki, S.; Tomiyasu, H. *Bull. Chem. Soc. Jpn. 65* (1992) 3022.

(77) Bányai, I.; Glaser, J.; Micdkei, K.; Tóth, I.; Zékány, L. *Inorg. Chem. 34* (1995) 3785.

(78) Szabó, Z.; Grenthe, I. *Inorg. Chem. 37* (1998) 6214.

(79) Ikeda, Y.; Soya, S.; Fukutomi, H.; Tomiyasu, H. *J. Inorg. Nucl. Chem 41* (1979) 1333.

(80) Wahlgren, U.; Moll, H.; Grenthe, I.; Schimmelphennig, B.; Maron, L.; Vallet, V.; Gropen, O. *J. Phys. Chem.* (submitted 1998).

(81) Wahlgren, U., personal communication.

(82) Yuchi, A.; Ban, T.; Wada, H.; Nakagawa, G. *Inorg. Chem. 29* (1990) 136.

(83) Shetty, S. Y.; Sathe, R. M. *J.inorg. Nucl. Chem. 39* (1977) 1837.

(84) Bogucki, R. F.; Martell, A. E. *J. Am. Chem. Soc. 80* (1958) 4170.

(85) Bottari, E.; Anderegg, G. *Helv. Chim. Acta 50* (1967) 2349.

(86) Nuttall, R. H.; Stalker, D. M. *Talanta 24* (1977) 355.